

TEMPORAL AGGREGATION BIAS AND MONETARY POLICY TRANSMISSION*

Margaret M. Jacobson[†] Christian Matthes[‡] Todd B. Walker[§]

March 2024

Abstract

Temporal aggregation can bias estimates of monetary policy transmission. Using impulse responses from both local projections and an unobserved components model, we find that the response of daily inflation to high-frequency monetary policy shocks confirms standard theoretical predictions. If there is an adversely-signed response such that inflation increases in response to a contractionary monetary policy shock, it is much more prominent when the dependent variables are aggregated to a lower frequency. We confirm these empirical findings in two data-generating processes that show how short-lived adversely-signed responses can be magnified when aggregating data to a lower frequency.

*This material reflects the views of the authors and not those of the Federal Reserve Board of Governors. The authors thank Miguel Acosta, Jonas Arias, and Francisco Ruge-Murcia for excellent discussions. Additionally, the authors thank Connor Brennan, Kairong Chen, and Jake Scott for excellent research assistance, as well as Sean D'Hoostelaere and seminar participants at Notre Dame, Osaka, the Federal Reserve Board, Bank of Canada Workshop on Monetary Policy Research, the Federal Reserve System Macro Meeting, the NBER Workshop on Methods and Applications for DSGE Models, the 25th Annual De Nederlandsche Bank Research Conference, Seoul National University, the Inaugural Macroeconometric Caribbean Conference, the Federal Reserve Bank of Cleveland, the University of Surrey, the King's College Macro Workshop, the Barcelona Summer Forum, the Society for Economic Dynamics Meeting, and the conference on New Challenges in Monetary Economics and Macro-Finance at the University of Mannheim for helpful comments. Finally the authors thank Miguel Acosta for help extending the Nakamura and Steinsson (2018a) shock series and John Rogers and Wenbin Wu for help reconstructing their shock series.

[†]Federal Reserve Board; Margaret.M.Jacobson@frb.gov

[‡]Department of Economics, Indiana University, matthesc@iu.edu

[§]Department of Economics, Indiana University, walkertb@indiana.edu

1 INTRODUCTION

This paper revisits a fundamental question of monetary economics: What is the transmission of monetary policy to the economy? Empirical work often finds that responses of macroeconomic variables to monetary policy shocks have the opposite sign of what standard theory predicts. Researchers trace these adversely-signed responses to information issues, with existing solutions consisting of either adding more variables [Sims (1992)] or emphasizing information mismatches between central banks and private sector agents as a “Fed information effect”.¹

We propose temporal aggregation bias—the information mismatch between the econometrician and private agents—as a new information-based explanation for the adversely-signed transmission of monetary policy. When using the daily CPI from the Billion Prices Project [Cavallo and Rigobon (2016)] as a temporally disaggregated macroeconomic indicator, we find that the adversely-signed response of inflation is short-lived, if it is present at all. A temporally disaggregated measure of inflation controls for temporal aggregation bias by aligning the frequencies of shocks and dependent variables and hence the information sets of the econometrician and private agents. We show that the frequency mismatches can account for the adversely-signed estimates of monetary policy transmission often found in existing work.

To understand how one can estimate a sizable adversely-signed response to monetary policy shocks with monthly or quarterly data but only a limited adversely-signed response with high-frequency data, we combine informal and formal empirical evidence with a simple model of temporal aggregation bias. We first establish that temporally aggregated high-frequency measures of inflation correlate well with official lower-frequency measures (e.g. monthly CPI) over our sample period (July 2008 to August 2015). Our empirical tests corroborate the claim that the high-frequency measure of inflation is “good at anticipating major *changes* in inflation *trends*,” [emphasis added, Cavallo and Rigobon (2016)].

Our main finding—the response of inflation is conventionally-signed with only a short-lived adversely-signed response if one is present at all—is obtained from the local projection specification advocated by Nakamura and Steinsson (2018b). The monetary policy shocks are identified via high-frequency variation in asset prices around monetary policy announcements, as is standard in the literature [Kuttner (2001), Gürkaynak et al. (2005), Campbell et al. (2012), Nakamura and Steinsson (2018a), Bu et al. (2021)]. We thus align the frequency of our variable of interest (inflation) more closely to the frequency of variation used to identify shocks. Impulse response functions show that although the response of inflation to a contractionary monetary policy shock is initially ambiguously positive for a few weeks, it is negative thereafter with 90% credible sets also below zero. By contrast, when inflation is time aggregated to a monthly frequency, impulse response functions show a significant impulse response that is positive.

Because the effect of temporal aggregation bias in local projections depends on the timing of high-frequency shocks, we build an unobserved components model that explicitly incorporates when monetary policy shocks occur within a month. This state space model adds the daily CPI and daily break-even

¹Bauer and Swanson (2023), Bu et al. (2021), and Caldara and Herbst (2019) also emphasize adding more information. For evidence and discussions of a Fed information effect see Romer and Romer (2000), Campbell et al. (2012, 2017), Nakamura and Steinsson (2018a), Jarocinski and Karadi (2020), Miranda-Agrippino and Ricco (2021), Lunsford (2020), Hoesch et al. (2023), Cieslak and Schrimpf (2019), Acosta (2023), Sastry (2022), Karnaukh and Vokata (2022), Lewis (2020), Bundick and Smith (2020), Andrade and Ferroni (2021), Golez and Matthies (2023), Nunes et al. (2023), Zhu (2023).

inflation rates as well as possible effects of monetary policy shocks into a model of inflation dynamics along the lines of Stock and Watson (2016) and Nason and Smith (2020). These impulse responses corroborate our local projection results by showing conventionally-signed transmission of monetary policy.

To shed light on our empirical estimates that uncover a conventionally-signed responses when frequencies of shocks and response variables are matched but adversely-signed responses when unmatched, we use two simple data generating processes to illustrate the effects of temporal aggregation bias. We first use Monte Carlo evidence to show how there is no clean identification of monetary policy transmission when time aggregating with local projections. Second, we use a well-known model from the monetary policy literature consisting of an Euler equation and a monetary policy rule to show how temporal aggregation can exacerbate initial impulse response functions.

Our contribution of temporal aggregation bias as an explanation for the adversely-signed transmission of monetary policy shocks provides further support for the ongoing claim, dating back to at least Kuttner (2001), that monetary policy needs to be studied in a high-frequency environment. Even though high-frequency economic indicators and temporal aggregation theory have been available for decades, we are the first—to our knowledge—to apply them to the study of monetary policy transmission.² By pairing high-frequency shocks with high-frequency response variables, our work follows existing specifications that estimate the transmission of monetary policy shocks to financial indicators.³ Financial indicators, however, may not be as susceptible to temporal aggregation bias as macroeconomic indicators because the former are observable at high frequencies. By contrast, economic indicators are accumulated over a fixed time interval and published with a lag, resulting in aggregation bias from potentially mismatched information sets between private agents observing high-frequency indicators and an econometrician relying on official releases.⁴

Unlike other studies, where competing methodologies or conditioning on different data serves to obfuscate analysis, a distinct advantage of our approach is the consistency in inference. We condition on the same data and apply the same methodology with the only distinction being the frequency of the data. An increase in the frequency of inflation observations eliminates adversely-signed monetary impulse responses. Because our temporal aggregation results are generic, we argue that the benefits of using high frequency data are neither limited to the study of monetary policy transmission nor prices and will be a key feature of the nascent field of high-frequency macro [Baumeister et al. (2021), Lewis et al. (2021)]. In a macroeconomic environment characterized by fast-moving turning points, such as the Great Financial Crisis or the COVID-19 recession, estimates of policy effects may be sensitive to the sampling frequency of economic response variables. Although high-frequency observables may be susceptible to measurement noise because they are only proxies of their lower frequency official counterparts, frameworks like our state space model allow for measurement error. We thus argue that measurement noise is not necessarily more important than the bias induced by temporal aggregation.

²Lewis et al. (2020a) discuss how time aggregation affects their estimates of monetary policy transmission to household expectations. See Shapiro et al. (2022), Aruoba et al. (2009), Lewis et al. (2020b) for other high frequency economic indicators.

³See Golez and Matthies (2023), Andrade and Ferroni (2021), Nakamura and Steinsson (2018a), Bauer and Swanson (2022), Gürkaynak et al. (2022), and Gürkaynak et al. (2021).

⁴For example, Stock and Watson (2007) note that time series estimates of the CPI are susceptible to temporal aggregation bias.

1.1 CONNECTION TO LITERATURE While Campbell et al. (2012) and Nakamura and Steinsson (2018a) find adversely-signed responses when estimating the transmission of high-frequency monetary policy shocks to lower frequency forecasts of macroeconomic aggregates, subsequent work finds that properly accounting for information delivers results that are either ambiguous or in line with structural predictions. Uribe (2022) takes a contrasting stance and argues that monetary policy shocks may actually be neo-Fisherian.

Closest to our specification of high-frequency inflation indicators responding to high-frequency monetary policy shocks are specifications that rely on commodity prices [Velde (2009)] or high-frequency expected inflation (TIPS) [Nakamura and Steinsson (2018a)]. Relative to these previously used proxies, we argue that the Billion Prices Project daily CPI is a relatively more complete measure of inflation and hence better suited to assess the transmission of monetary policy shocks. Commodities are known to be more volatile than measures of inflation which may result in different sensitivities to monetary policy shocks. Similarly, the responses of expected and realized inflation to monetary policy shocks may differ because the former tends to be anchored while the latter is more prone to fluctuations. Common specifications that rely on the change in Blue Chip forecasts may thus be understating the transmission of monetary policy shocks to inflation because they capture changes in expected rather than current inflation. By contrast, we posit that the different sensitivities of expectations and actual indicators is less of an issue for the transmission of monetary policy shocks to GDP or other real indicators.

Although Buda et al. (2023) also estimate the response of high-frequency economic indicators to high-frequency monetary policy shocks, they focus on transmission lags rather than the effects of frequency mismatches. Using high-frequency data on Spanish consumption, sales, and unemployment along with monetary policy shocks from European Central Bank announcements, this work similarly finds conventionally-signed impulse responses without prominent adverse signs. The consistency of our findings with theirs is striking given the differences in indicators (prices vs. quantities) and economies (US vs. EU). Furthermore, our theoretical and Monte-Carlo based analysis highlights how temporal aggregation can emerge as an important source of bias when estimating the effects of monetary policy and can account for the responses of both papers.⁵

Rather than following much of the empirical monetary policy transmission literature and focusing on information refinements to possible explanatory variables, we instead follow Bauer and Swanson (2023) and contribute refinements to the less-studied measurement of response variables. Because Bauer and Swanson's (2023) survey finds that Blue Chip forecasters rarely change their estimates of economic indicators in response to monetary policy announcements, alternative response variables such as high-frequency indicators may prove useful. The literature's focus on explanatory variables stems from several studies finding predictability and or bias in standard high-frequency monetary policy shocks such as those estimated by Nakamura and Steinsson (2018a). These studies mainly focus on the response of GDP and argue that the adverse sign disappears once the shocks are either orthogonalized [Karnaukh and Vokata (2022), Bauer and Swanson (2022)] or conditioned on missing information [Caldara and Herbst

⁵Grigoli and Sandri (2022) relatedly explore the transmission of high-frequency ECB monetary policy shocks to high-frequency German credit card data and corroborate conventionally-signed responses.

(2019), Sastry (2022), Miranda-Agrippino and Ricco (2021), Bauer and Swanson (2023)].

Many studies—including Nakamura and Steinsson (2018a)—account for the adversely-signed transmission of high-frequency monetary policy shocks by appealing to Romer and Romer’s (2000) Fed information effect, which argues that central banks have an information advantage over private agents.⁶ For example, in response to tighter monetary policy private agents revise up their forecasts of inflation because they perceive a signal that the central bank has relatively optimistic non-public information. Other papers find that controlling for central bank information advantages affects estimates of monetary policy transmission [Lunsford (2020), Bu et al. (2021), Hoesch et al. (2023), Cieslak and Schrimpf (2019), Nunes et al. (2023), Zhu (2023)] or eliminates adversely-signed responses entirely [Miranda-Agrippino and Ricco (2021), Jarocinski and Karadi (2020)]. In fact, Acosta (2023) and Lewis (2020) identify Fed information shocks and find evidence that is either mixed or against adversely-signed monetary policy transmission.

In contrast these existing studies, we do not explicitly test or model how the information sets of central banks and private agents account for our conventionally-signed estimates of monetary policy transmission. We instead focus on the less-studied but complementary information mismatch between private agents and the econometrician to account for conventionally-signed estimates of monetary policy transmission with high-frequency data, but adversely-signed estimates with time-aggregated data.

Decades of work support our claim that temporal aggregation bias can affect both the direction and magnitude of estimates of monetary policy transmission. We follow Marcet (1991) in demonstrating how the systematic effect of time aggregation can bias the first few coefficients of the moving-average representation. Coupled with results in Amemiya and Wu (1972), who show that temporal aggregation of autoregressive processes preserves invertibility, these biases would infiltrate modern approaches to VAR identification. This puts our main result—that adversely-signed estimates of monetary policy transmission can be explained by temporal aggregation bias—on firm theoretical ground. While applications of these ideas in applied macroeconomics are still relatively rare, Forni and Marcellino (2016) highlight how jointly using data collected at different frequencies can help with the identification of structural VARs with a focus on traditional recursive identification schemes, whereas Forni and Marcellino (2014) make a similar argument for dynamic equilibrium models. Christiano and Eichenbaum (1987) highlight the impact temporal aggregation can have using two examples in macroeconomics. A related, but distinct, literature has developed tools to estimate regression-type models when the left-hand side is sampled at a different frequency than the right hand side (Ghysels et al., 2004).

2 HIGHER-FREQUENCY OBSERVATIONS AND INFLATION DYNAMICS

We first demonstrate that a high-frequency inflation proxy can contain information obfuscated by the publication lags of official series. Our analysis uses the Billion Prices Project Daily Price Index (BPP).

⁶Faust et al. (2004) find that the adversely-signed response of inflation disappears once the Volcker disinflation is excluded from Romer and Romer’s (2000) study. Similarly, Sastry (2022), Bundick and Smith (2020) and Bauer and Swanson (2023) explicitly test for a central bank information advantage and find no evidence.

Several papers have already established the ability of the BPP to improve forecasts of the CPI [Cavallo and Rigobon (2016), Aparicio and Bertolotto (2020) and Harchaoui and Janssen (2018)]. We also refer readers to these papers for a detailed discussion of BPP construction. Our analysis below confirms that the BPP contains *additional* information that is obfuscated by the official CPI’s publication lags over our sample period.⁷

2.1 DAILY INFLATION DATA We define daily inflation as the 30-day percentage change in the BPP, which allows for the units of daily inflation to be comparable to those of official inflation which are measured at monthly frequency. The BPP is constructed from over five million online prices from 300 retailers in 50 countries webscraped daily. While we provide a brief overview here, a meticulous description of the data is provided in Cavallo and Rigobon (2016). Our data consists of (publicly available) observations from 2008 to 2015. Advantages of the data are [i.] the higher frequency (daily) vis-a-vis the CPI (monthly or bi-monthly) or scanner data (weekly); and [ii.] the number of prices collected far exceeds the CPI (500k vs. 80k). The disadvantages are [i.] prices are only collected from online retailers and therefore the sample is not representative of all consumer prices; specifically, the sample contains no pricing from the services sector.⁸ According to Cavallo and Rigobon (2016), the data contain at least 70 percent of the weights in Consumer Price Index (CPI) baskets of roughly 25 countries; [ii.] Because prices are webscraped, the data does not contain information on quantities sold. Thus, online prices must be coupled with weights from consumer expenditure surveys or other sources to yield expenditure-weighted data.⁹ Even though prices obtained by physically visiting stores may not necessarily coincide with those observed online, Cavallo (2017) finds a 70 percent match rate.

2.2 CONNECTION TO THE CPI To alleviate concerns that BPP data may not align well with the US CPI, we now conduct several tests to show that the BPP can contain additional information obfuscated by the official CPI’s publication lags, a fact that we will exploit in our econometric analysis.

Statistic	Release delay (days)
Mean	16.97
Standard error	2.73
Min	13
Max	30

Table 1: Summary statistics on CPI release delays from July 2008 to August 2015.

⁷See Appendix E for specific details on the series used including seasonal adjustment.

⁸Although comparing the BPP to a version of the CPI with the same coverage of categories would be an ideal exercise, we are limited by data availability. We have instead repeated some of the calculations of this section using sub-categories of the CPI and the results are broadly similar as shown in Appendix A. These sub-categories include the commodity price index, the commodity plus shelter index, the official index less energy, and the official index less medical services. Although we focus on comparing the BPP to the CPI because the former is constructed from the weights of the later, we also compare the BPP to the PCE index. In fact table 6 shows that the BPP’s Nowcast of the PCE has an R^2 that is similar to that of the CPI. The reported Nowcast coefficient of the PCE specification is much lower than its CPI counterpart which likely can be attributed to the different weights used in construction.

⁹The BPP only discloses weights pooled across all countries where they collect data. They do not disclose country specific weights. See <https://www.pricesstats.com/approach/data-composition>.

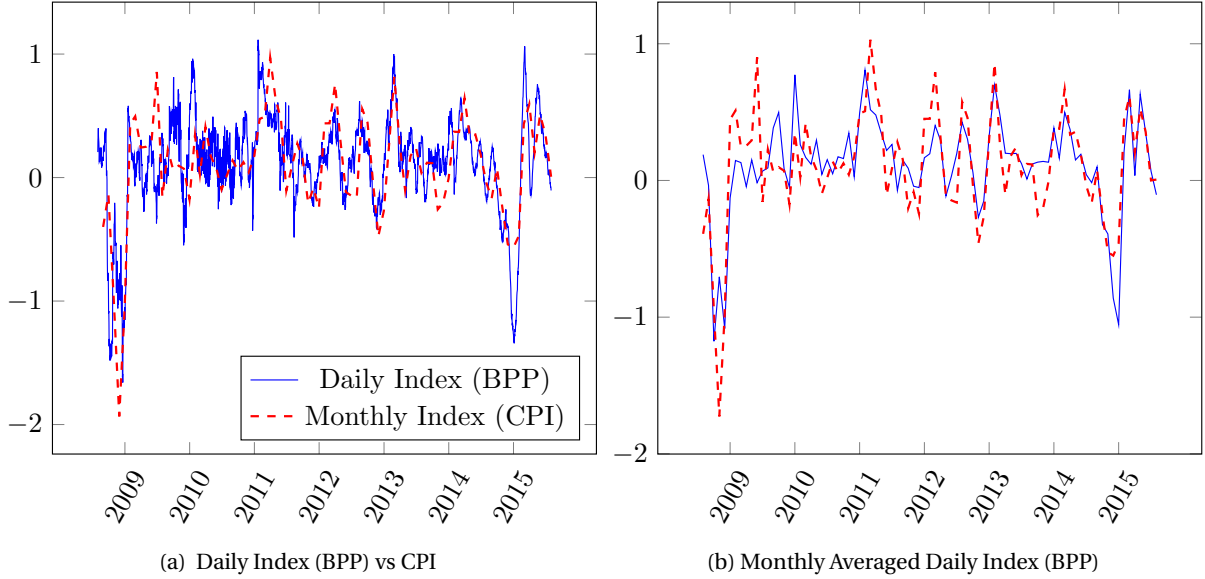


Figure 1: Official and daily inflation, monthly and 30-day percentage change. For month T , $\Delta CPI_T = 100 \times (\log CPI_T - \log CPI_{T-1})$ and for day t , $\Delta BPP_t = 100 \times (\log BPP_t - \log BPP_{t-30})$ so that $\Delta BPP_T = \frac{1}{m} \sum_{t=1}^m 100 \times (\log BPP_t - \log BPP_{t-30})$ for $t = 1, \dots, m$ days in month T .

Panel 1a plots the percentage change of the monthly CPI and the BPP daily index; panel 1b plots the percentage change of the monthly CPI against the aggregated monthly BPP. While the correlation of the two series plotted in panel 1b is only 0.63, several studies have shown that the BPP index is particularly adept at picking up turning points in the CPI, which leads to improved forecasts [Cavallo and Rigobon (2016), Aparicio and Bertolotto (2020) and Harchaoui and Janssen (2018)]. To show this result holds over our sample period, we use the monthly aggregated BPP series to conduct a Nowcast of the CPI by estimating, $\Delta CPI_T = \beta_0 + \beta_1 \Delta BPP_T + e_T$. Despite both indices being denoted with subscript T , the CPI at date T is announced with a slight delay as shown by Table 1, which documents the summary statistics of release delays in days (e.g., June 2008 CPI was released July 16). Given that our interest lies in high-frequency changes in inflation, the slight difference in timing is relevant as one can use the monthly average of the BPP to predict that month's CPI number. The estimated value is 0.94 with an R-squared of 0.58, implying substantial predictive power as shown in panel 2b. Panel 2a plots the in-sample predicted values against the realized values.

Given the persistence of inflation, we address the following question: Is there any *additional* predictive power of the BPP beyond that contained in past values of the CPI? Table 2 compares the Nowcast to an autoregressive representation of the CPI. Column one reports the AR(1) specification results. Columns two and three condition only on past values of the BPP, and show a substantial increase in the R-squared value when conditioning on the contemporaneous BPP, while the lagged BPP has less predictive content than last month's CPI. Columns four and five demonstrate an affirmative answer to the question of additional predictive power of the BPP: The coefficients on the contemporaneous BPP are positive and

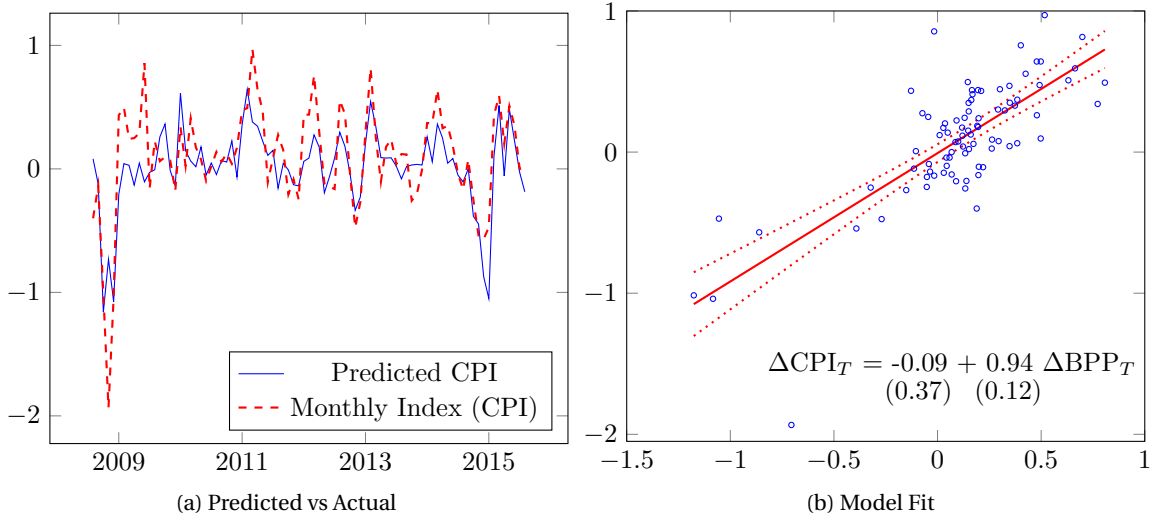


Figure 2: Nowcast of CPI using monthly aggregated BPP, monthly percentage change. Standard errors in parentheses on panel 2b. For month T , $\Delta CPI_T = 100 \times (\log CPI_T - \log CPI_{T-1})$ and for day t and month T , $\Delta BPP_T = \frac{1}{m} \sum_{t=1}^m 100 \times (\log BPP_t - \log BPP_{t-30})$ for $t = 1, \dots, m$ days in month T .

statistically significant. The R-squared value is twice as high as the autoregressive specification.¹⁰

	ΔCPI_T				
	(1)	(2)	(3)	(4)	(5)
ΔCPI_{T-1}	0.558*** (0.143)				0.178 (0.107)
ΔBPP_T		0.937*** (0.129)		0.878*** (0.097)	0.828*** (0.106)
ΔBPP_{T-1}			0.591** (0.248)	0.109 (0.193)	-0.030 (0.222)
R^2	0.32	0.58	0.23	0.59	0.61
Adj. R^2	0.31	0.58	0.22	0.58	0.60

Standard errors in parentheses. * ($p < .10$), ** ($p < .05$), *** ($p < .01$)

Table 2: Nowcast of BPP vs. autoregressive CPI. For month T , $\Delta CPI_T = 100 \times (\log CPI_T - \log CPI_{T-1})$ and for day t and month T , $\Delta BPP_T = \frac{1}{m} \sum_{t=1}^m 100 \times (\log BPP_t - \log BPP_{t-30})$ for $t = 1, \dots, m$ days in month T .

3 EMPIRICAL RESULTS

Given that the BPP index can contain information obfuscated by the official CPI's publication lags, the next phase of the analysis asks how the index responds to monetary policy and whether this response is different at a daily or monthly frequency. High-frequency identification methods that exploit variation

¹⁰We conduct several robustness checks in Appendix A which corroborate our findings that the BPP index is effective at predicting changes in inflation. For example, we construct alternative metrics for computing inflation (levels, end-of-month values) and examine different types of seasonality (day-of-the-week).

in asset prices around monetary policy announcements have become the standard in the literature [e.g., Kuttner (2001), Gürkaynak et al. (2005), Campbell et al. (2012), Nakamura and Steinsson (2018a), Bu et al. (2021)]. Using high-frequency inflation data allow us to align the dependent variable with the independent variables, and to the best of our knowledge, we are the first to do so. Our expectation here is *not* that inflation jumps immediately (within the day) in response to surprise changes in interest rates, but that prices could substantially change by the time the CPI is made publicly available.

3.1 MEASURES OF HIGH-FREQUENCY MONETARY POLICY SHOCKS Before estimating monetary policy transmission with disaggregated inflation data, we briefly describe our choice of monetary policy shocks and their respective timing and identification. We discuss two such constructions in detail—Nakamura and Steinsson (2018a) (NS) and Bu et al. (2021) (BRW). We focus on these shocks because they are characterized by a single factor that can be parsimoniously embedded into more complex frameworks like our state space model. Even though the NS shock is widely used, there are known concerns about predictability and bias. For this reason, we also include estimates using the BRW shock as it claims to control for some of these concerns.

NS define a “policy news shock” as the first principal component of the change in five interest rate futures around a 30-minute window of FOMC announcements. These futures span the first year of the term structure and include the expected federal funds rate at the end of the month of the FOMC announcement, the expected federal funds rate at the end of the month of the next scheduled FOMC announcement, and expected 3-month Eurodollar interest rates at horizons of two, three and four quarters. Together, these futures capture the effects of surprise changes in the federal funds rate and forward guidance. Our extension of this shock series is constructed from the Chicago Mercantile Exchange Datamine futures tick data to assure as close of a match as possible to the original series. BRW use a Fama and MacBeth (1973) two-step regression to extract unobserved monetary policy shocks from the common component of zero-coupon yields encompassing the full yield curve. The first step estimates the responsiveness of yields of different maturities to monetary policy via standard time-series regressions. Filtering out non-monetary policy news is done through the heteroskedasticity-based estimator of Rigobon (2003) and Rigobon and Sack (2004), implemented by employing instrumental variables (IV). We construct both of these shock series ourselves using underlying asset pricing data, see Brennan et al. (2024) for details and additional analysis.

Figure 3 plots monetary policy shock series for each method over our sample period. As noted in BRW, their shock series has “moderately high correlation” with that of NS in addition to those of Swanson (2021) and Jarocinski and Karadi (2020). What is evident from the figure is that the BRW shock series has much more dispersion because it better captures the expansive 21st century monetary policy toolkit as explained in Brennan et al. (2024) and Bu et al. (2021).

3.2 LOCAL PROJECTIONS We use local projections (Jorda, 2005) to estimate the impulse responses of inflation to monetary policy shocks at both daily and monthly frequencies. For the daily specification, let y_{t+h} be the value of daily inflation over the past 30 days at day $t+h$, z_t be the high-frequency shock series proxying for exogenous variation in monetary policy, and x_{t-1} be the vector of controls, which are

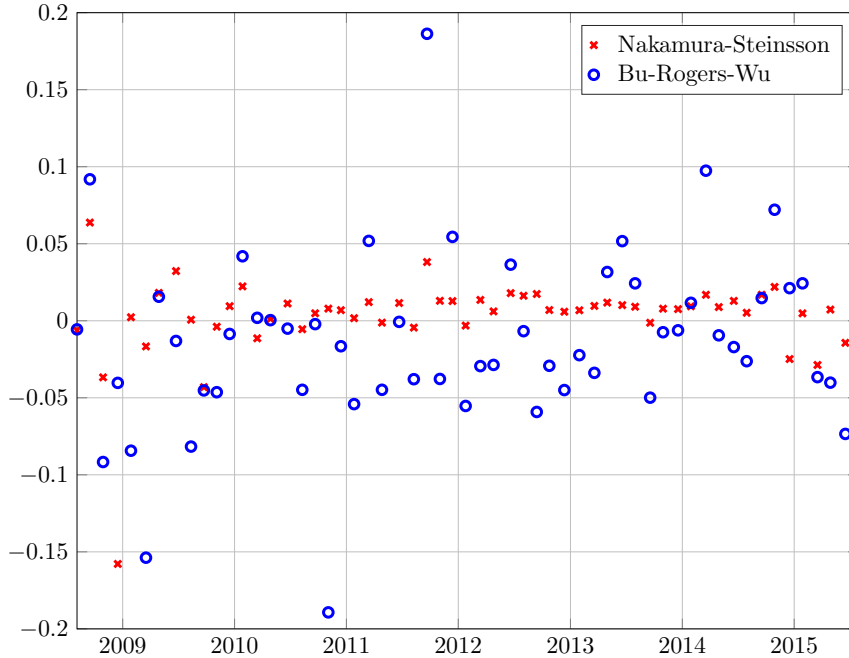


Figure 3: Monetary policy shock series from Nakamura and Steinsson (2018a) and Bu et al. (2021). Authors' construction.

30 lags of daily inflation. We estimate

$$y_{t+h} = \alpha_{(h)} + \beta_{(h)}x_{t-1} + \Gamma_{(h)}z_t + e_t^{(h)}, \quad e_t^{(h)} \sim N(0, \sigma_{(h)})$$

with robust heteroskedasticity and autocorrelation consistent (HAC) standard errors. We normalize the high-frequency monetary shock series proxying for exogenous variation in monetary policy to have unit variance for either frequency and then plot impulse responses that raise the instrument by one standard deviation. We use either the aforementioned series from Nakamura and Steinsson (2018a) or Bu et al. (2021). The model specification at monthly frequency simply aggregates daily data via an arithmetic average and includes a lag of monthly data as controls to be comparable.

Figure 4 plots the impulse response to a one-time contractionary NS monetary policy shock at both the daily and monthly frequency. Panel 4a shows daily inflation responds positively initially; however, the 90% confidence interval substantially overlaps zero for periods zero through 33. After roughly 30 periods (one month), the inflation response turns negative and is significantly so for the remaining days shown. At a daily frequency, the NS shock sequence does not produce a substantial and long-lasting positive response of inflation to a contractionary monetary policy shock. The magnitude of the initial positive response is roughly half that of the negative (and much more persistent) response. Panel 4b aggregates the daily index to a monthly frequency.¹¹ When inflation is aggregated to a monthly frequency, the initial

¹¹There is only one month in our sample with two monetary policy announcements suggesting little potential for bias from

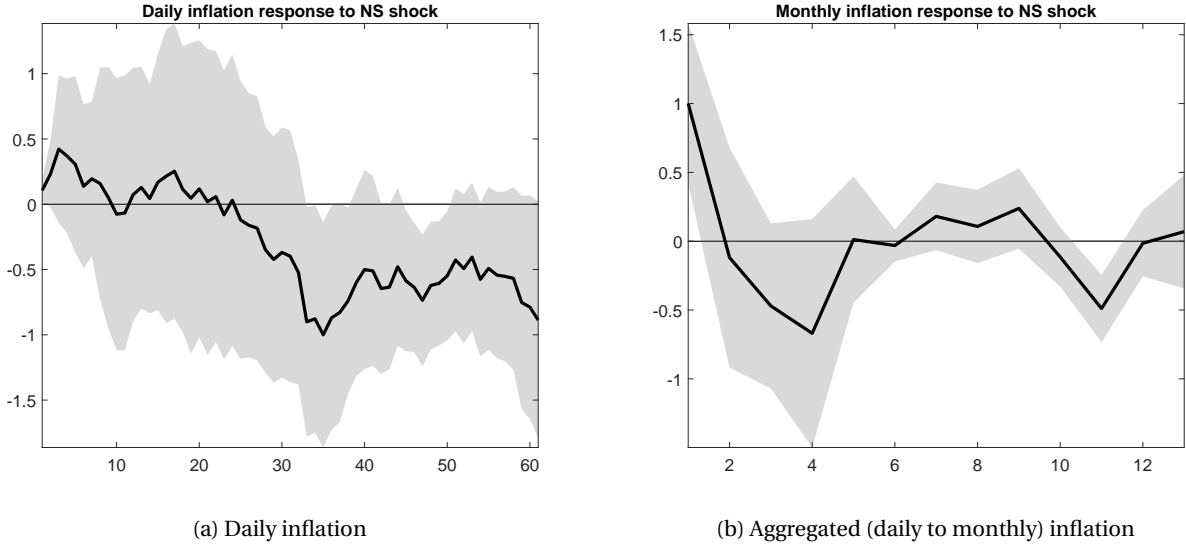


Figure 4: Impulse response of daily inflation (30-day percentage change) to a one standard deviation Nakamura and Steinsson (2018a) shock: aggregated vs disaggregated. For a given month, the aggregated series are the sum of the monetary policy shocks and the average of 30-day percentage change of daily inflation, $BPP_T = \frac{100}{m} \sum_{t=1}^m (\log BPP_t - \log BPP_{t-30})$ for days $t = 1, \dots, m$ of month T . Error bands are 90 %.

positive response is quantitatively large and one of the few components of the impulse response function for which the confidence band does not cover zero. Although a prominent positive response is often found in the literature, it contrasts our findings of a negative and significant response using disaggregated daily inflation.

Figure 5 plots the impulse response of inflation to a contractionary BRW monetary policy shock. Panel 5a shows that, at daily frequency, the median response of inflation is close to zero or slightly negative until about period 60 (two months) when it becomes more negative and on the margin of the confidence bands. In contrast, when the daily index is aggregated to a monthly frequency, the point estimate of the impact response is positive, albeit zero is well contained in the 90% credible sets. Given that the Fed information effect and its associated adversely-signed responses are not detected in the BRW shock, the results plotted in figure 5 are not surprising.

3.3 DISCUSSION The monthly / aggregated *positive* response of inflation to a *contractionary* NS monetary policy shock plotted in panel 4b behooves researchers to provide an explanation. Standard theory tells us that a contractionary shock should reduce inflation. This adversely-signed response to monetary policy shocks that we find in panel 4b is a robust finding of the empirical literature while the conventionally-signed response in panel 4a is relatively novel.

One explanation for what we refer to as an adversely-signed response is the Fed information effect's notion that private agents react to the novel information revealed in monetary policy announcements.¹²

the aggregation / scaling of high-frequency monetary policy shocks.

¹²Romer and Romer (2000), Campbell et al. (2012, 2017), Nakamura and Steinsson (2018a), Jarocinski and Karadi (2020),

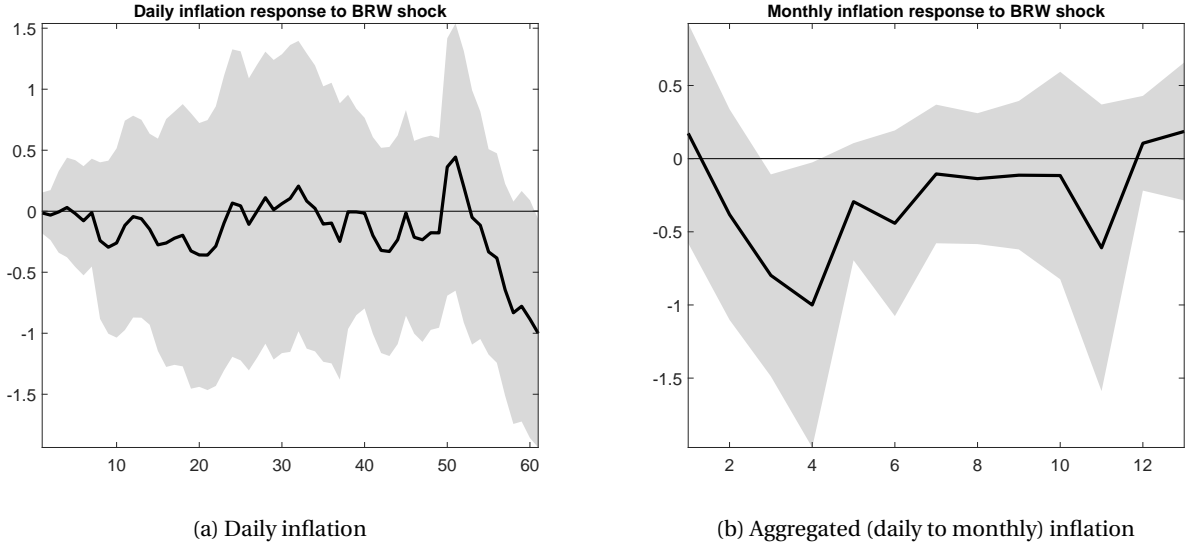


Figure 5: Impulse response of daily inflation (30-day percentage change) to a one standard deviation Bu et al. (2021) shock: aggregated vs disaggregated. For a given month, the aggregated series are the sum of the monetary policy shocks and the average of 30-day percentage change of daily inflation, $BPP_T = \frac{100}{m} \sum_{t=1}^m (\log BPP_t - \log BPP_{t-30})$ for days $t = 1, \dots, m$ of month T . Error bands are 90 %.

Thus, a response that runs counter to standard theory could be explained by introducing a discrepancy in information between the Federal Reserve and private agents, as advocated by Nakamura and Steinsson (2018a). However, testing for this effect requires high frequency data. Previous studies [e.g., Jarocinski and Karadi (2020), Lunsford (2020)] examined the reaction of asset prices, such as stocks and bonds, but we are the first to study inflation at high frequency. Figure 4 demonstrates that the adversely-signed response to inflation could be due to an information discrepancy between the econometrician and private agents, and not just the Federal Reserve and private agents. At the daily frequency, no such adversely-signed response materializes. Temporal aggregation can explain the significant and positive initial response in aggregated data when no such response is present at higher-frequency. We explore this conjecture more thoroughly in Section 4.

Moreover, in Brennan et al. (2024) we show that a conventionally-signed impulse response of daily inflation is robust to other monetary policy shock series—like those of Kuttner (2001) and Jarocinski and Karadi (2020)—in addition to those of Nakamura and Steinsson (2018a) and Bu et al. (2021) shown here. Furthermore, Appendix B shows that the impulse response of daily inflation are conventionally-signed to the federal funds rate target shock of Gürkaynak et al. (2005) but adversely-signed to the forward guidance path shock. If the NS shock can be interpreted as the linear combination of the target and path shocks, we find that the impulse responses to the distinct components are exactly as one would expect.

Miranda-Agrippino and Ricco (2021), Lunsford (2020), Hoesch et al. (2023), Cieslak and Schrimpf (2019), Acosta (2023), Lewis (2020), Bundick and Smith (2020), Andrade and Ferroni (2021), Golez and Matthies (2023).

3.4 UNOBSERVED COMPONENTS MODEL An unobserved components model allows us to study the response of high-frequency inflation to a monetary policy shock more systematically by taking into account the exact timing of monetary policy shocks and official inflation releases within a month. We employ this methodology for several reasons. First, the permanent-transitory decompositions cast in state space form have proven very useful for inflation at lower frequencies [Stock and Watson (2020)]. Second, there is transparency in modeling assumptions. Relative to the local projections methodology, the modeling assumptions here are more straightforward. This allows us to take a more definitive stance on our finding of a conventionally-signed estimate of monetary policy transmission, as opposed to disentangling how temporal aggregation might interact with, say, our IV estimation. Third and relatedly, the model specification is parsimonious. Finally and most importantly, the state space / estimation methodologies allow us to more easily handle data observed at different frequencies and with observations missing at different dates—we use daily inflation data, data on break-even inflation rates that are available daily except for holidays and weekends, infrequent monetary policy shocks, and monthly inflation rates.

#	Parameter	Prior	Notes
1	σ_π	$\Gamma(1, 0.5)$	standard deviation of i.i.d. component of underlying inflation
2	σ_τ	$\Gamma(1, 0.5)$	standard deviation of innovation to random walk permanent component
3	ρ_g	$\beta(4, 4)$	persistence of stationary part
4	σ_g	$\Gamma(1, 0.5)$	standard deviation of innovation to stationary part
5	α^m	$N(0, 0.0001^2)$	intercept of measurement equation of monthly CPI inflation
6	$\sigma^{monthly}$	$\Gamma(1, 0.5)$	standard deviation of measurement error of monthly CPI inflation
7	α^{daily}	$N(0, 5^2)$	intercept of measurement equation of daily (30-day) inflation
8	σ^{daily}	$\Gamma(1, 0.5)$	standard deviation of measurement error of daily inflation
9	α^{BE}	$N(0, 5^2)$	intercept of measurement equation of daily BE inflation
10	σ^{BE}	$\Gamma(1, 0.5)$	standard deviation of measurement error of daily BE inflation
11	θ_0^g	$N(0, 0.25^2)$	contemporaneous impact of monetary policy shock on g
12	θ_0^τ	$N(0, 0.25^2)$	contemporaneous impact of monetary policy shock on τ
13	$\sigma^{m,obs}$	$\Gamma(1, 0.5)$	standard deviation of monetary policy shock
14 ~ 72	θ_i^g 59×1	$N(0, (0.25 * 0.95^i)^2)$	vector of effects of 59 days lagged monetary policy shocks on g
73 ~ 131	θ_i^τ 59×1	$N(0, (0.25 * 0.95^i)^2)$	vector of effects of 59 days lagged monetary policy shocks on τ

Table 3: Prior Specification

Our model consists of the following state equations:

$$\begin{aligned} \pi_t &= \tau_t + g_t + e_t^\pi && \text{Unobserved daily CPI inflation} \\ \tau_t &= \tau_{t-1} + \sum_{k=0}^K \theta_k^\tau m_{t-k} + e_t^\tau && \text{Permanent component} \\ g_t &= \rho g_{t-1} + \sum_{j=0}^J \theta_j m_{t-j} + e_t^g && \text{Transitory component} \end{aligned}$$

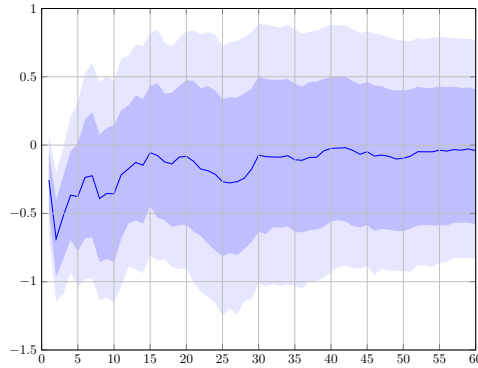
The permanent component of inflation allows for a unit-root specification and a sequence of monetary policy shocks for 60 periods ($K = J = 60$). The transitory component permits auto-correlation and the same number of monetary policy shocks. We assume monetary policy shock dynamics $m_t = e_t^m$ with all

shocks e being i.i.d. and Gaussian.¹³

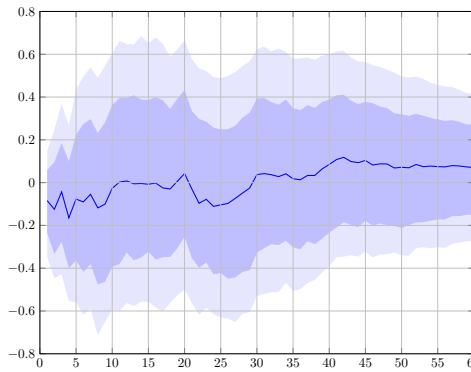
The observation equations are:

$$\begin{aligned} \pi_t^m &= \alpha^m + \pi_{t-p} + e_t^{monthly} && \text{Monthly observation of CPI} \\ \pi_t^{daily} &= \alpha^{daily} + \pi_t + e_t^{daily} && \text{Daily measure of 30-day inflation} \\ \pi_t^{BE,h} &= \alpha^{BE} + E_t \pi_{t,t+h} + e_t^{BE} && \text{10-year break-even rates} \end{aligned}$$

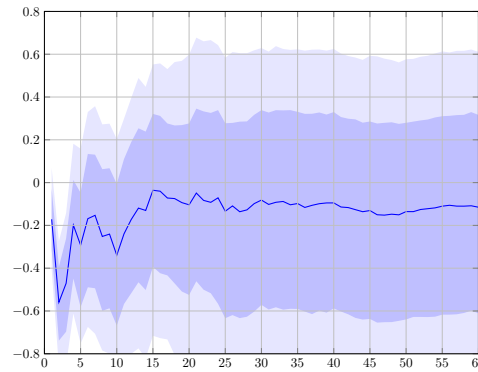
where p is the publication lag mentioned in Section 2 (which can vary over time as shown in Table 1). We assume that high-frequency monetary policy shock series are a noisy measurement of the true exogenous variation in monetary policy: $m_t^{obs} = m_t + e_t^{m,obs}$, along the lines of Caldara and Herbst (2019). Note that the model implies $E_t \pi_{t+h} = E_t(\tau_{t+h} + g_{t+h}) = \tau_t + \rho^h g_t \approx \tau_t$, where the last approximation is imposed on the estimation procedure (our prior imposes that the daily persistence of the transitory component $|\rho| < 1$, and h represents the 10-year horizon).



(a) Overall Impulse Response



(b) Response of Transitory Component (g_t)



(c) Response of Permanent Component (τ_t)

Figure 6: Impulse responses to a one standard deviation Nakamura and Steinsson (2018a) monetary policy shock. Error bands are 68 % and 90 % posterior bands centered at the median.

¹³In contrast to previous work using state space models to describe inflation dynamics, we explicitly incorporate a role for monetary policy shocks. We allow these shocks (which are measured with error) to affect both transitory and permanent components of inflation. This is important because movements in inflation that might seem permanent at the daily frequency can correspond to persistent, but non-permanent components at a lower frequency.

The estimation is Bayesian with the likelihood function evaluated using the Kalman filter. To effectively explore the posterior distribution, a sequential Monte Carlo algorithm is implemented [Herbst and Schorfheide (2016)]. We use 15,000 particles with 200 steps to go from the prior to the full posterior and five Metropolis Hastings steps per iteration of the algorithm. Table 3 reports our prior distributions, which are largely uninformative. We do impose somewhat informative priors on the effects of monetary policy shocks on the transitory and permanent components of inflation. We center those priors at 0 to not bias our results for or against finding adversely-signed responses, but we do impose shrinkage—the further a monetary policy shock is in the past, the more we shrink its effect toward zero. These findings are robust to imposing less shrinkage as shown in Appendix C.

Panel 6a plots the overall impulse response function of inflation to a contractionary NS monetary policy shock, while panels 6b-6c plot the response of the transitory and permanent components, respectively.¹⁴ Darker shaded error bands are 68th percentiles, while lighter shades are 90th. Panel 6a shows that inflation—at a daily frequency—does not contain an adversely-signed response. The initial reaction of inflation to a one standard deviation monetary policy shock is negative, even at the 90th percentile, followed by an increase and an error band that contains zero over the remaining horizon. These results further corroborate our findings from the local projections; namely, that the adversely-signed response of inflation to a monetary policy shock is difficult to detect when controlling for the information sets of the econometrician and private agents.

By decomposing into permanent and transitory components, we are able to parse the conventionally-signed impulse response as permanent. Panel 6c shows a conventionally-signed impulse response in the permanent component of daily inflation. The less-persistent transitory response is shown to be quantitatively small relative to trend as shown in panel 6b. The variance decomposition, shown in figure 7, shows that the lion’s share of volatility is explained by the permanent component of inflation as opposed to the transitory component. Taken together, these figures suggest that methodologies that de-trend inflation prior to analysis could miss conventionally signed responses. More germane to our argument, the transitory component *when evaluated at daily frequencies* does not display a substantial adversely-signed response despite the fact that the shocks fed into the system are known to generate adversely-signed responses at much lower (monthly) frequencies.

3.5 DISCUSSION To summarize, our empirical findings suggest that temporal aggregation, going from daily observations of inflation to monthly, can generate impulse response functions that are qualitatively different. Using the Nakamura and Steinsson (2018a) shock series, we find a positive response of inflation to a contractionary monetary policy shock at the monthly frequency, yet no such positive response emerges at daily frequency. We verify these findings by estimating a flexible unobserved components model that allows for permanent and transitory components. At daily frequency, the transitory response is negligible, while the permanent component reacts in a manner consistent with theory (inflation falls in response to a contractionary shock). We now turn to theory to address how such outcomes are possible.

¹⁴Results are similar for the BRW shock series and are available upon request.

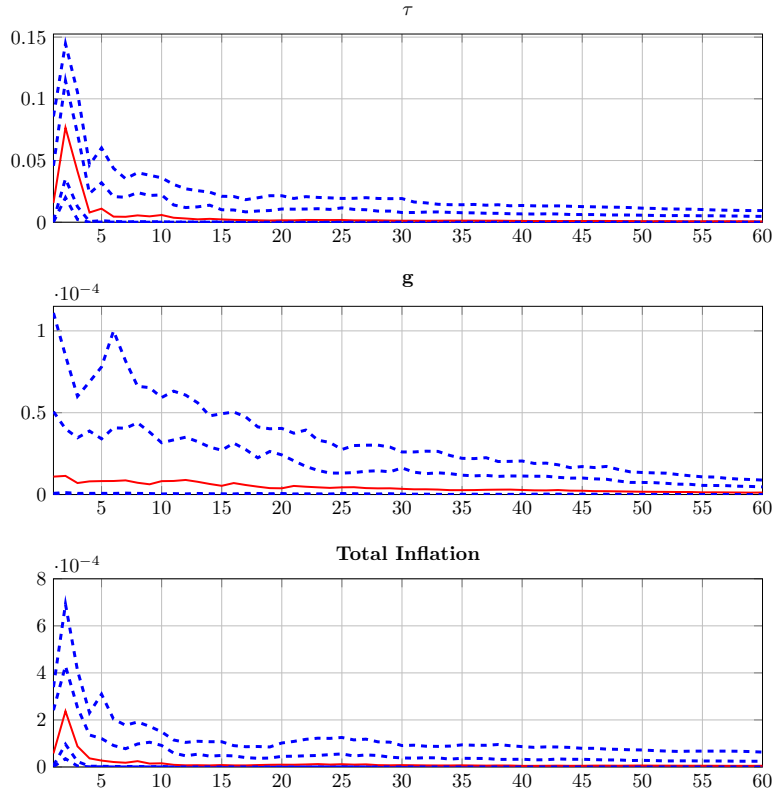


Figure 7: Variance decomposition associated with monetary policy shock as a fraction of total variance.

4 UNDERSTANDING TEMPORAL AGGREGATION

We employ stylized models of monetary policy to show how properties of temporal aggregation can account for our empirical results of Section 3. Using simulated data and local projections, we show how a short-lived adversely-signed response (i.e., positive response of inflation to a contractionary monetary policy shock) can seep into lower frequencies due to temporal aggregation bias. We then provide a more theoretical framework to demonstrate *how* temporal aggregation leads to substantial bias in impulse response functions; specifically, in the initial values of moving-average representations. We keep the models sufficiently simple in order to provide clear intuition, acknowledging that these are examples as opposed to theorems. However, we conjecture robustness of our results by appealing to an earlier literature that operates in continuous time.

4.1 TEMPORAL AGGREGATION WITH LOCAL PROJECTIONS Consider the data-generating process of inflation,

$$\pi_t = \sum_{j=0}^{59} \Theta_j \varepsilon_{t-j}^{mp} + u_t \tag{1}$$

$$u_t = \rho^u u_{t-1} + \varepsilon_t^u$$

where t is assumed to be daily, and the monetary policy shock $\varepsilon_t^{mp} \sim N(0, 1)$ is uncorrelated with the persistent shock $u_t \sim N(0, \sigma_u^2)$. We assume the monetary policy shock occurs only once per month, while u_t occurs every day. We examine three alternative specifications of the timing of the monetary policy shock—a shock that occurs at the beginning (day 1), middle (day 15), and end (day 30) of the month. To approximate population moments, we simulate three million daily observations, taking 30-day averages of shocks and the inflation process (1) to obtain corresponding monthly data. We denote monthly variables as Π_T and ε_T^{mp} , where T is measured in months. Local projections are used to estimate monthly responses of inflation to the monetary policy shock, controlling for lagged inflation outcomes. We set $\rho_u = 0.99$ and $\sigma_u = 1$ to capture the idea that other shocks are just as important as monetary policy for the evolution of inflation at the daily frequency. The parameters governing the reaction of inflation to monetary policy are given by $\Theta_j = 1$ for $j = 0, \dots, 9$ and $\Theta_j = -1$ for $j = 10, \dots, 59$. Our calibration is consistent with the local projection response of daily inflation to the NS shock series shown in figure 4.

Our parameterization accomplishes two tasks: first, it introduces what we refer to as an initial adversely-signed policy response of inflation; that is, the first ten daily observations of inflation following a monetary policy shock are inconsistent with standard theory in that a contractionary shock would lead to an increase in inflation. Second, the average effect over the 30-day period is consistent with theory. The remaining two-thirds of the daily observations over the month enter with a negative coefficient, implying a contractionary shock would lead to a fall in inflation. Note also that the magnitudes of the first 10 days and last 20 days are similar. The implication of our calibration is that one would *not* expect the adversely-signed inflationary response to materialize in the aggregate (monthly) data because a majority of the signs—20 out of 30—are negative instead of positive. The short-lived adversely-signed response should essentially be dominated by the theoretically-consistent response.

Table 4 shows results for three local projection specifications and various timing of the monetary policy shock. In two of the three specifications, the econometrician would find a *positive* initial response of inflation to a monthly monetary policy shock, despite the fact that the time-averaged response is negative. Only when the monetary policy shock hits towards the beginning of the month does the sign of the response of inflation match the temporally aggregated negative value. The lagged shock, ε_{T-1} , does enter with a negative sign, so while the initial response could be adversely-signed, the subsequent moves are standard.

The timing of the monetary policy shock is important. Figure 8 (left panel) plots the time-aggregated monthly moving average coefficients (i.e. the accumulated response to a monetary policy shock) (left, y-axis) against the timing of the monetary policy shock (x-axis).¹⁵ The time-aggregated MA coefficients

¹⁵Note that this accumulated response is not directly comparable to our estimates reported in table 4 since we assume in

	Panel A: Beginning			Panel B: Middle			Panel C: End		
	ε_T^{mp}	Π_{T-1}	ε_{T-1}^{mp}	ε_T^{mp}	Π_{T-1}	ε_{T-1}^{mp}	ε_T^{mp}	Π_{T-1}	ε_{T-1}^{mp}
Π_T	-0.40	0.82		0.29	0.82		0.03	0.82	
Π_T	-0.50		-1.16	0.38		-0.85	-0.06		-0.26
Π_{T+1}	-1.09	0.61		-0.92	0.60		-0.19	0.60	

Table 4: Local projection results. Three million observations of daily inflation simulated via (1) and aggregated to monthly (30 day) frequency were estimated using local projections. The panels denote when the monetary policy shock hits the economy, at the beginning (day 1), middle (day 15) or end (day 30) of the month. Dependent variables are in the first column, the other columns display the coefficients of the right-hand-side variable given at the top of each column within a panel. The first row of the results is the response of inflation to the monetary policy shocks from the current and previous months. The second and third row of results are the local projections at time $T = 0$ and $T = 1$, respectively.

for any month can be written as $\Psi \equiv \sum_{t=0}^{29-j} (\mathbb{1}_{t \leq 9} - \mathbb{1}_{t > 9})$ where $j = 29, \dots, 0$ is the day of the month when the monetary policy shock occurs. For example, when $j = 29$ the shock occurs on the last day of the month and $\Psi = 1$. As j decreases, the shock occurs earlier in the month, and the monthly aggregated response Ψ becomes larger. In fact, the largest positive response $\Psi = 10$ is on day $j = 21$. Thereafter, the negative MA coefficients enter into the monthly aggregation and the largest negative impact $\Psi = -10$ is when the shock occurs on day $j = 0$ at the very beginning of the month. The histogram plotted on the left panel of figure 8 shows that over our sample period, the timing of FOMC announcements is consistent with the shock hitting during the middle of the month. The mean and median FOMC announcement occurred on the 19th day of the month, and a majority of the announcements occurred after the 10th day of the month. This simple example shows how researchers using aggregated data can estimate a positive response of inflation to a contractionary monetary policy shock even though most of the disaggregated response coefficients are negative.¹⁶

Finally, we note that the results are not contingent on the parameterization of the daily process, u_t . Figure 8 (right panel) plots the initial response using the middle of the month timing as in panel B of table 4 against the serial correlation coefficient and standard deviation. It shows that size of the positive coefficient in the LP regression is increasing in the correlation of the non-monetary policy shock and its standard deviation, but remains substantial (0.13) when these values are close to zero. These results confirm our empirical findings—a short-lived adversely-signed response at daily frequency can be persistent and significant at monthly frequency.

4.2 DISCUSSION It is important to emphasize how we define “bias” in this example. Of course, the econometrician would be better off using high-frequency data to estimate the response of inflation to a monetary policy shock. They would find an adversely-signed positive response that is quickly dominated

our simulations that there is only one monetary policy shock per month and in practice there are eight scheduled FOMC announcements per year.

¹⁶Typically the FOMC meeting schedule is set years in advance. Although unscheduled FOMC announcements do occur, they are quite rare and there is only one such announcement in our sample. It is therefore possible that the day of the month of an FOMC announcement is random, but unlikely in practice.

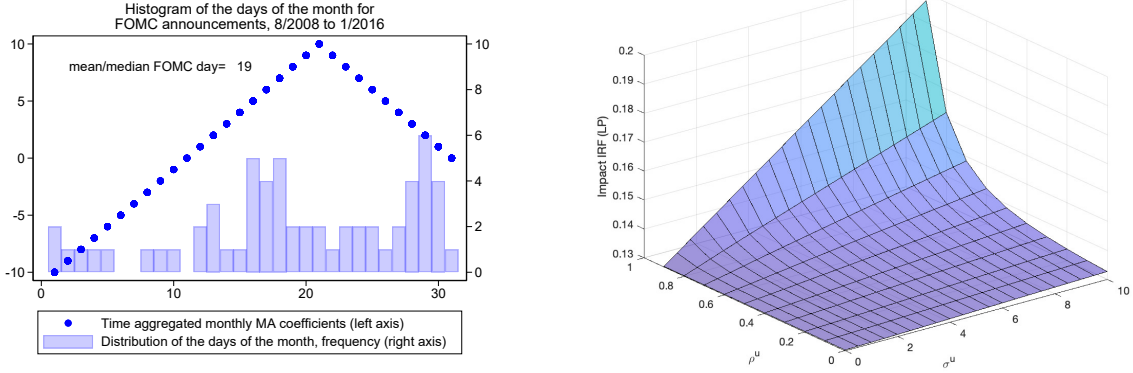


Figure 8: Robustness. Accumulated responses as a function of shock timing (left panel) and impact IRFs estimated via local projections as a function of autocorrelation (ρ^u) and standard deviation (σ^u) (right panel).

by the negative response, consistent with the local projection impulse response of panel 4a. However, suppose only temporally aggregated data are available. One would expect the negative terms to dominate the temporal aggregation, eliminating the initial positive impulse response of monthly inflation. This does not happen in panel 4b and it does not happen in our simulation, hence the term temporal aggregation bias. Thus, we have generated a simulation consistent with our empirical findings. The final section addresses *how* such a result can occur.

4.3 TEMPORAL AGGREGATION IN A STRUCTURAL MODEL We now provide a more theoretical framework to demonstrate how temporal aggregation leads to substantial bias in impulse response functions. Consider a nominal bond that costs \$1 at date t and pays off $(1 + i_t)$ at date $t + 1$. The asset-pricing equation for this bond can be written in log-linearized form as a Fisher equation, $i_t = r + \mathbb{E}[\pi_{t+1}|I_t]$, where the real interest rate is assumed to be constant and $\mathbb{E}[\pi_{t+1}|I_t]$ is the private agents' expectation of next period's ($t + 1$) inflation. Monetary policy follows a Taylor rule, adjusting the nominal interest rate in response to inflation, $i_t = r + \phi[\pi_t|I_t] + x_t$, where the monetary policy shock follows an AR(1) process, $x_t = \rho x_{t-1} + \varepsilon_t$, with $\rho \in (0, 1)$ and ε_t distributed as Gaussian with mean zero and variance σ_ε^2 . We assume the information set of the monetary authority is consistent with private agents' (I_t) so that we can isolate the effects of the information mismatch between private agents and the econometrician. The unique equilibrium rate of inflation is well known and follows from implementing the Taylor principle ($\phi > 1$),

$$\pi_t = -\frac{x_t}{\phi - \rho} = \rho\pi_{t-1} + w_t \quad (2)$$

where $w_t = -\varepsilon_t/(\phi - \rho)$.

We assume the econometrician observes realizations of the equilibrium processes at a frequency that is lower than private agents. Specifically, let $t = mT$ and define the temporally aggregated inflation

	$m = 1$	$m = 2$	$m = 5$	$m = 10$	$m = 20$	$m = 30$	$m = 40$	$m = 50$
ρ^m	0.990	0.980	0.951	0.904	0.818	0.740	0.669	0.605
θ	0.000	0.171	0.250	0.264	0.265	0.266	0.266	0.267
σ_u^2	0.028	0.041	0.085	0.160	0.288	0.391	0.476	0.542
σ_Π^2	1.397	1.389	1.374	1.351	1.307	1.266	1.226	1.186

Table 5: Estimates of the ARMA(1,1) equation (4) using temporally aggregated observations of equation (2). Note that for $m = 1$ (no temporal aggregation), $\sigma_u^2 = \sigma_w^2$.

process as

$$\Pi_T = \left(\frac{1}{m}\right) \left(\sum_{j=0}^{m-1} L^j\right) \pi_{mT} = \left(\frac{1}{m}\right) (\pi_{mT} + \pi_{mT-1} + \dots + \pi_{mT-m+1}) \quad T = 1, 2, 3, \dots \quad (3)$$

For example, if t is a month and $m = 3$, then T is a quarter. Inflation, π_t , could be interpreted as a monthly year-over-year percentage change, and the three-month non-overlapping arithmetic mean is one possible way of aggregating. Alternatively, we could assume to observe month-over-month inflation and the direct summation yields quarterly inflation. Our analysis below is robust to these alternative aggregation methods.

Appendix D shows that temporally aggregating the AR(1) inflation process given by (2) yields an ARMA(1,1) representation,

$$(1 - \rho^m L)\Pi_T = u_T + \theta u_{T-1} \quad u_T \sim N(0, \sigma_u^2) \quad (4)$$

where, for lag operator L , the autocorrelation coefficient is raised to the power of m (the number of aggregated components), and the estimated shocks (u_t) will be fundamental for the Π_t process (Amemiya and Wu (1972)). The last fact ensures that an autoregressive (or VAR) representation will accurately estimate the ARMA process. An analytical mapping between the aggregated inflation process and the ARMA(1,1) parameters is not feasible but Table 5 provides estimates of the parameters for various values of m using simulated data. We set $\rho = 0.99$, $\phi = 1.05$, $\sigma_\varepsilon^2 = 0.01$, and use one million disaggregated observations.

The estimates in Table 5 reveal important properties of the mapping between an AR(1) process and its temporally aggregated ARMA(1,1) counterpart: [i.] the autocorrelation coefficient decays exponentially at rate m ; [ii.] the variance of the aggregate inflation process declines multiplicatively in m (see Appendix D for derivation).

$$\sigma_\Pi^2 = \frac{\sigma_u^2}{m^2} (m + 2[(m-1)\rho + (m-2)\rho^2 + \dots + \rho^{m-1}]) \quad (5)$$

Taken together, [i] and [ii] imply that the variance of the innovation process σ_u^2 and the moving average parameter θ must compensate for the faster decline in the autocorrelation coefficient, ρ^m . Table 5 shows that the variance of the innovation (σ_u^2) increases 46% for $m = 2$ and by a factor of ten for $m = 20$, and the moving-average parameter also increases with m . The increase in the estimated variance will translate

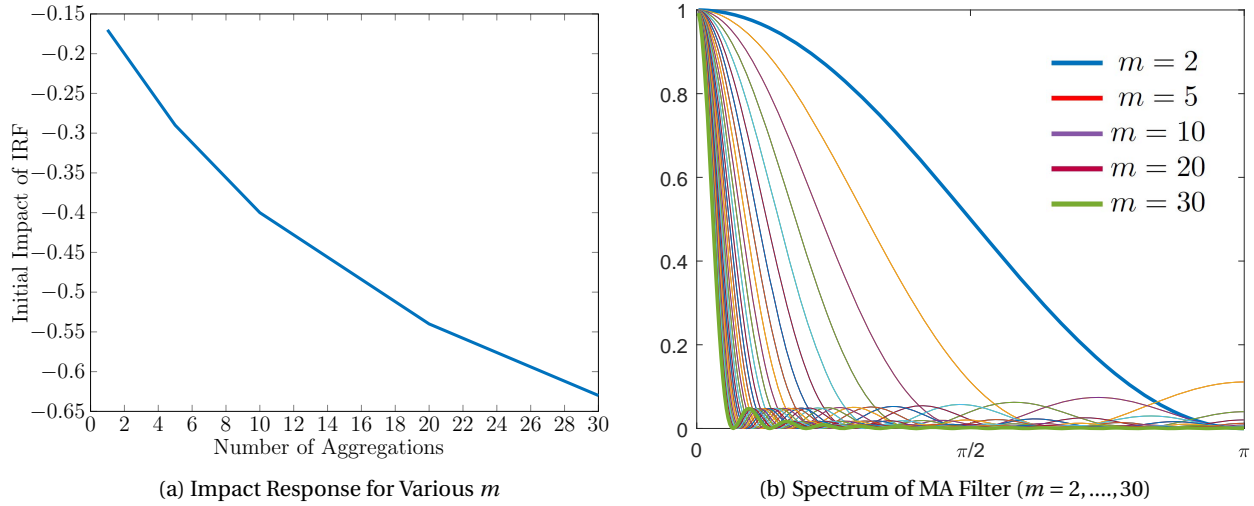


Figure 9: Initial impulse response and moving-average filter for various m . Panel a (left-side) shows the decline in the initial impact coefficient as m increases from 1 to 30. Panel b (right-side) plots the spectrum for $m = 2$ (blue) through $m = 30$ (green), demonstrating why low frequency properties are preserved.

into a more pronounced *initial* impact of the impulse response of inflation to a monetary policy shock. Panel 9a plots the initial impulse response to a one-standard deviation shock (σ_u) for various levels of aggregation. Note that the units of the x-axis correspond to the degree of aggregation m . The disaggregated impulse ($m = 1$) shows an inflation process with an impact response that is substantially mitigated relative to the temporally aggregated responses. Even a slight increase in the degree of aggregation leads to a substantial change in the impact response to a monetary policy shock—temporally aggregating over six periods more than doubles the initial impact. This dynamic is consistent with our empirical findings in Section 3, specifically figures 4 and 5.¹⁷

Panel 9b plots the moving-average filter $(\frac{1}{m}) \left(\sum_{j=0}^{m-1} L^j \right)$ in the frequency domain over the range of 0 to π . The panel shows that a MA filter is a low-pass filter, allowing lower frequencies to pass through while attenuating medium and higher frequencies. What is critical for understanding the bias associated with temporal aggregation is *how* the reallocation of the spectrum is distributed across various parameters of the estimated ARMA(1,1) process. Lower frequencies are preserved when aggregation occurs despite the decline in the autocorrelation coefficient (from ρ to ρ^m). Amemiya and Wu (1972) show that, for any stationary AR(p) representation, temporal aggregation preserves the order of the autoregressive process (i.e., an AR(p) becomes an ARMA(p,q))¹⁸ with the autoregressive roots all raised to the power m . These seemingly conflicting properties—a decline in the value of the (positive) autocorrelation roots coupled with no subsequent change in the low frequency properties of the time series process—leads to a substantial change in the initial impulse response coefficients through an increase in the variance of the

¹⁷One distinction between this exercise and our empirics is the normalization of the variance. If one were to normalize the variance for the temporally aggregated series to match the disaggregated value, the correction would come through the moving average term and figure 9 continues to be relevant.

¹⁸Stram and Wei (1986) show this condition holds as long as the AR roots are distinct from the MA roots.

innovation process and appearance of positive moving-average parameters.

4.4 DISCUSSION The purpose of this section was to establish how temporal aggregation can substantially alter initial moving-average coefficients. An econometrician time-aggregating the data will attribute a structural interpretation to a significant adversely-signed initial reaction of inflation to a monetary policy shock, when the lion's share of the response is due to temporal aggregation bias. While we believe this section has established compelling intuition for our results, the models are stylized and so we briefly discuss robustness. Appealing to Marcet (1991), our primary result is not an artifact of specific assumptions underlying our model but is due to the more generic properties of temporal aggregation. Working in a continuous-time framework and with generic Wold representations, Marcet (1991) finds the “systematic effect of time aggregation is to increase the absolute size of the *first few coefficients* of the MAR (moving-average representation) (emphasis added).” This result, coupled with the fact that temporal aggregation preserves invertibility for autoregressive processes (Amemiya and Wu (1972)), suggests that our results are robust to alternative specifications.

5 CONCLUDING THOUGHTS

This paper revisits a fundamental question of monetary economics: What is the transmission of monetary policy to the economy? We introduce temporal aggregation bias as a new information-based explanation for the adversely-signed transmission of monetary policy shocks. When using the daily CPI from the Billion Prices Project as a temporally disaggregated macroeconomic indicator, we find a conventionally-signed response with only a short-lived adverse sign when present at all. To understand how one can obtain a sizable adversely-signed response to monetary policy shocks with monthly or quarterly data when only a limited adversely-signed response is found at a higher frequency, we combine informal and formal empirical evidence with a simple model of temporal aggregation bias. Because our temporal aggregation results are generic, and macroeconomic indicators are published with a lag, we argue that temporal aggregation bias is not limited to our study of monetary policy transmission and will likely be a key feature of the nascent field of high-frequency macro.

REFERENCES

- Acosta, Miguel**, “The Perceived Causes of Monetary Policy Surprises,” 2023. Working Paper.
- Amemiya, Takeshi and Roland Y. Wu**, “The Effect of Aggregation on Prediction in the Autoregressive Model,” *Journal of the American Statistical Association*, 1972, 67 (339), 628–632.
- Andrade, Philippe and Filippo Ferroni**, “Delphic and Odyssean Monetary Policy Shocks: Evidence from the Euro Area,” *Journal of Monetary Economics*, 2021, 117, 816–832.
- Aparicio, Diego and Manuel I. Bertolotto**, “Forecasting inflation with online prices,” *International Journal of Forecasting*, 2020, 36 (2), 232–247.
- Aruoba, S. Boragan, Francis X. Diebold, and Chiara Scotti**, “Real-Time Measurement of Business Conditions,” *Journal of Business and Economic Statistics*, 2009, 27 (4), 417–427.
- Bauer, Michael D. and Eric T. Swanson**, *A Reassessment of Monetary Policy Surprises and High-Frequency Identification*, University of Chicago Press, March 2022.
- **and —**, “An Alternative Explanation for the “Fed Information Effect,”” *American Economic Review*, March 2023, 113 (3), 664–700.
- Baumeister, Christiane, Danilo Leiva-León, and Eric Sims**, “Tracking Weekly State-Level Economic Conditions,” *Review of Economics and Statistics*, 2021.
- Brennan, Connor M., Margaret M. Jacobson, Christian Matthes, and Todd B. Walker**, “Monetary Policy Shocks: Data or Methods?,” 2024. Working Paper.
- Bu, Chunya, John Rogers, and Wenbin Wu**, “A unified measure of Fed monetary policy shocks,” *Journal of Monetary Economics*, 2021, 118, 331–349.
- Buda, G., V. M. Carvalho, G. Corsetti, J. B. Duarte, S. Hansen, A. S. Moura, A. Ortiz, T. Rodrigo, A. Ortiz, and A. Ortiz**, “Short and Variable Lags,” Cambridge Working Papers in Economics 2321, Faculty of Economics, University of Cambridge March 2023.
- Bundick, Brent and A. Lee Smith**, “The Dynamic Effect of Forward Guidance Shocks,” *Review of Economics and Statistics*, 2020, 102 (5), 946–965.
- Caldara, Dario and Edward Herbst**, “Monetary Policy, Real Activity, and Credit Spreads: Evidence from Bayesian Proxy SVARs,” *American Economic Journal: Macroeconomics*, 2019, 11 (1), 157–192.
- Campbell, Jeffery R., Charles L. Evans, Jonas D. M. Fisher, and Alejandro Justiniano**, “Macroeconomic Effects of Federal Reserve Forward Guidance,” *Brookings Papers on Economic Activity*, 2012, pp. 1–54.
- Campbell, Jeffrey R., Jonas D. M. Fisher, Alejandro Justiniano, and Leonardo Melosi**, “Forward Guidance and Macroeconomic Outcomes since the Financial Crisis,” *NBER Macroeconomics Annual*, 2017, 31, 283–357.

- Cavallo, Alberto**, “Are Online and Offline Prices Similar? Evidence from Multi-Channel Retailers,” *American Economic Review*, 2017, 107.
- **and Roberto Rigobon**, “The Billion Prices Project: Using Online Data for Measurement and Research,” *Journal of Economic Perspectives*, 2016, 31 (1).
- Christiano, Lawrence J. and Martin Eichenbaum**, “Temporal aggregation and structural inference in macroeconomics,” *Carnegie-Rochester Conference Series on Public Policy*, 1987, 26, 63–130.
- Cieslak, Anna and Andreas Schrimpf**, “Non-monetary News in Central Bank Communication,” *Journal of International Economics*, 2019, 118, 293–315.
- Fama, Eugene F. and James D. MacBeth**, “Risk, Return, and Equilibrium: Empirical Tests,” *Journal of Political Economy*, 1973, 81 (3), 607–636.
- Faust, Jon, Eric Swanson, and Jonathan H. Wright**, “Identifying VARs Based on High Frequency Futures Data,” *Journal of Monetary Economics*, 2004, 51 (6), 1107–1131.
- Forni, Claudia and Massimiliano Marcellino**, “Mixed-Frequency Structural Models: Identification, Estimation, And Policy Analysis,” *Journal of Applied Econometrics*, November 2014, 29 (7), 1118–1144.
- **and –**, “Mixed frequency structural vector auto-regressive models,” *Journal of the Royal Statistical Society Series A*, February 2016, 179 (2), 403–425.
- Ghysels, Eric, Pedro Santa-Clara, and Rossen Valkanov**, “The MIDAS Touch: Mixed Data Sampling Regression Models,” University of California at Los Angeles, Anderson Graduate School of Management qt9mf223rs, Anderson Graduate School of Management, UCLA June 2004.
- Golez, Benjamin and Ben Matthies**, “Fed Information Effects: Evidence from the Equity Term Structure,” 2023. Working Paper.
- Grigoli, Francesco and Damiano Sandri**, “Monetary Policy and Credit Card Spending,” 2022. Working Paper.
- Gürkaynak, Refet S., A. Hakan Kara, Burcin Kisaçikoğlu, and Sang Seok Lee**, “Monetary Policy Surprises and Exchange Rate Behavior,” *Journal of International Economics*, 2021, 130.
- **, Brian P. Sack, and Eric T. Swanson**, “Do Actions Speak Louder than Words? The Response of Asset Prices to Monetary Policy Actions and Statements,” *International Journal of Central Banking*, 2005, 1, 55–93.
- **, Hatice Gökçe Karasoy-Can, and Sang Seok Lee**, “Stock Market’s Assessment of Monetary Policy Transmission: the Cash Flow Effect,” 2022. *Journal of Finance*, forthcoming.
- Harchaoui, Tarek M. and Robert V. Janssen**, “How can big data enhance the timeliness of official statistics? The case of the U.S. consumer price index,” *International Journal of Forecasting*, 2018, 34, 225–234.

- Herbst, Edward and Frank Schorfheide**, *Bayesian Estimation of DSGE Models*, 1 ed., Princeton University Press, 2016.
- Hoesch, Lukas, Barbara Rossi, and Tatevik Sekhposyan**, “Has the Information Channel of Monetary Policy Disappeared? Revisiting the Empirical Evidence,” *American Economic Journal: Macroeconomics*, July 2023, 15 (3), 355–87.
- Jarocinski, Marek and Peter Karadi**, “Deconstructing Monetary Policy Surprises: The Role of Information Shocks,” *American Economic Journal: Macroeconomics*, 2020, 12 (2).
- Jorda, Oscar**, “Estimation and Inference of Impulse Responses by Local Projections,” *American Economic Review*, March 2005, 95 (1), 161–182.
- Karnaukh, Nina and Petra Vokata**, “Growth forecasts and news about monetary policy,” *Journal of Financial Economics*, 2022, 146 (1), 55–70.
- Kuttner, Kenneth N.**, “Monetary Policy Surprises and Interest Rates: Evidence from the Fed Funds Futures Market,” *Journal of Monetary Economics*, 2001, 47, 523–544.
- Lewis, Daniel, Christos Makridis, and Karel Mertens**, “Do Monetary Policy Announcements Shift Household Expectations?,” 2020. Working Paper.
- Lewis, Daniel J.**, “Announcement-Specific Decompositions of Unconventional Monetary Policy Shocks and Their Macroeconomic Effects,” 2020. Federal Reserve Bank of New York Staff Reports, no. 891.
- Lewis, Daniel, Karel Mertens, Jim Stock, and Mihir Trivedi**, “High Frequency Data and a Weekly Economic Index During the Pandemic,” *American Economic Association Papers and Proceedings*, 2021, 111.
- , **Karl Mertens, and James Stock**, “U.S. Economic Activity During the Early Weeks of the SARS-Cov-2 Outbreak,” *COVID Economics*, 2020, 1 (6), 1–21.
- Lunsford, Kurt**, “Policy Language and Information Effects in the Early Days of Federal Reserve Forward Guidance,” *American Economic Review*, 2020, 110, 2899–2934.
- Marcet, Albert**, “Temporal Aggregation of Economic Time Series,” in Lars P. Hansen and Thomas J. Sargent, eds., *Rational Expectations Econometrics*, Boulder, CO: Westview Press, 1991, pp. 237–281.
- Miranda-Agrippino, Silvia and Giovanni Ricco**, “The Transmission of Monetary Policy Shocks,” *American Economic Journal: Macroeconomics*, July 2021, 13 (3), 74–107.
- Nakamura, Emi and Jón Steinsson**, “High-Frequency Identification of Monetary Non-Neutrality: The Information Effect,” *Quarterly Journal of Economics*, 2018, 133, 1283–1330.
- **and** – , “Identification in Macroeconomics,” *Journal of Economic Perspectives*, 2018, 32 (3), 59–86.

- Nason, Jim and Gregor W. Smith**, “Measuring the Slowly Evolving Trend in U.S. Inflation with Professional Forecasts,” *Journal of Applied Econometrics*, 2020, 36, 1–17.
- Nunes, Ricardo, Ali Ozdagli, and Jenny Tang**, “Interest Rate Surprises: A Tale of Two Shocks,” 2023. Discussion Papers 2320, Centre for Macroeconomics (CFM).
- Rigobon, Roberto**, “Identification Through Heteroskedasticity,” *The Review of Economics and Statistics*, 11 2003, 85 (4), 777–792.
- **and Brian Sack**, “The impact of monetary policy on asset prices,” *Journal of Monetary Economics*, 2004, 51 (8), 1553–1575.
- Romer, Christina D. and David H. Romer**, “Federal Reserve Information and the Behavior of Interest Rates,” *American Economic Review*, 2000, (90), 429–457.
- Sastry, Karthik A.**, “Disagreement About Monetary Policy,” 2022. working paper.
- Shapiro, Adam Hale, Moritz Sudhof, and Daniel J. Wilson**, “Measuring news sentiment,” *Journal of Econometrics*, 2022, 228 (2), 221–243.
- Sims, Christopher**, “Interpreting the macroeconomic time series facts: The effects of monetary policy,” *European Economic Review*, 1992, 36 (5), 975–1000.
- Stock, James and Mark Watson**, “Why Has U.S. Inflation Become Harder to Forecast?,” *Journal of Money, Credit and Banking*, 2007, 39.
- **and _**, “Core Inflation and Trend Inflation,” *Review of Economics and Statistics*, 2016, 98 (4), 770–784.
- **and _**, “Slack and Cyclically Sensitive Inflation,” *Journal of Money, Credit and Banking*, 2020, 52.
- Stram, Daniel O. and William W.S. Wei**, “Temporal Aggregation in the ARIMA Process,” *Journal of Time Series Analysis*, 1986, 7 (4), 279–292.
- Swanson, Eric T.**, “Measuring the effects of federal reserve forward guidance and asset purchases on financial markets,” *Journal of Monetary Economics*, 2021, 118, 32–35.
- Uribe, Martín**, “The Neo-Fisher Effect: Econometric Evidence from Empirical and Optimizing Models,” *American Economic Journal: Macroeconomics*, 2022, 14, 133–162.
- Velde, François R.**, “Chronicle of a Deflation Unforetold,” *Journal of Political Economy*, 2009, 117 (4), 591–634.
- Wei, William W.S. and Mohammad Ahsanullah**, “The Effects of Time Aggregation on the AR(1) Process,” *Computational Statistics Quarterly*, 1984, 1, 343–352.
- Zhu, Linyan**, “Let the Market Speak: Using Interest Rates to Identify the Fed Information Effect,” 2023. Working Paper.

A APPENDIX: BPP ROBUSTNESS CHECKS

A.1 ALTERNATIVE CONSTRUCTIONS OF BPP INFLATION This section shows an alternative version of figure 2.

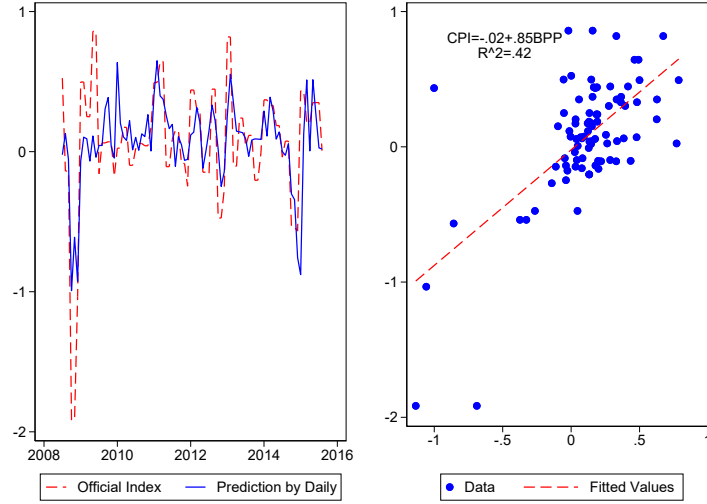


Figure 10: Nowcast of CPI using end of month values of the BPP, monthly and 30-day percentage change. For month T , $\Delta CPI_T = 100 \times (\log CPI_T - \log CPI_{T-1})$ and for day m of month T , $\Delta BPP_T = 100 \times (\log BPP_m - \log BPP_{m-30})$.

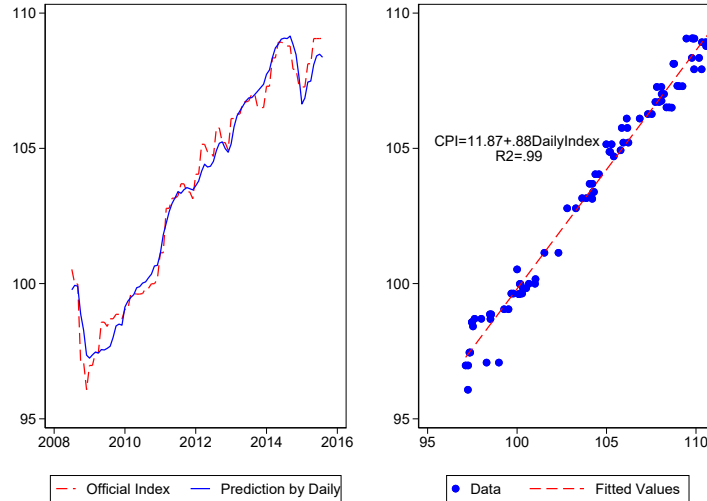


Figure 11: Nowcast of CPI using aggregated monthly values of the BPP index. For month T , $CPI_T = \log CPI_T$ and for day t of month T , $\Delta BPP_T = \frac{1}{m} \sum_{t=1}^m \log BPP_t$ for $t = 1, \dots, m$ days in month T .

A.2 CPI SUB-CATEGORIES Table 6 shows how the BPP Nowcast of the headline CPI compares to other CPI sub-categories and the PCE index.

	ΔCPI_T^i , sub-categories i					ΔPCE_T
	(1)	(2)	(3)	(4)	(5)	(6)
	Headline	Commodities	Commodities & Shelter	Headline ex energy	Headline ex Medical	Headline PCE
ΔBPP_T	0.937*** (0.129)	1.618*** (0.283)	0.530*** (0.121)	0.180*** (0.052)	1.001*** (0.137)	0.497*** (0.081)
R^2	0.58	0.48	0.36	0.21	0.59	0.52
Adj. R^2	0.58	0.47	0.36	0.20	0.58	0.52

Standard errors in parentheses. * ($p < .10$), ** ($p < .05$), *** ($p < .01$)

Table 6: Nowcast of CPI sub-categories using the BPP. For month T and sub-category i , $\Delta CPI_T^i = 100 \times (\log CPI_T^i - \log CPI_{T-1}^i)$; for day t and month T , $\Delta BPP_T = \frac{1}{m} \sum_{t=1}^m 100 \times (\log BPP_t - \log BPP_{t-30})$ for $t = 1, \dots, m$ days in month T ; and for month T , $\Delta PCE_T = 100 \times (\log PCE_T - \log PCE_{T-1})$.

A.3 SEASONALITY

$$BPP_t = trend_t + \sum_j \alpha_j^{day} \mathbf{1}_{day\ of\ week} + \epsilon_t$$

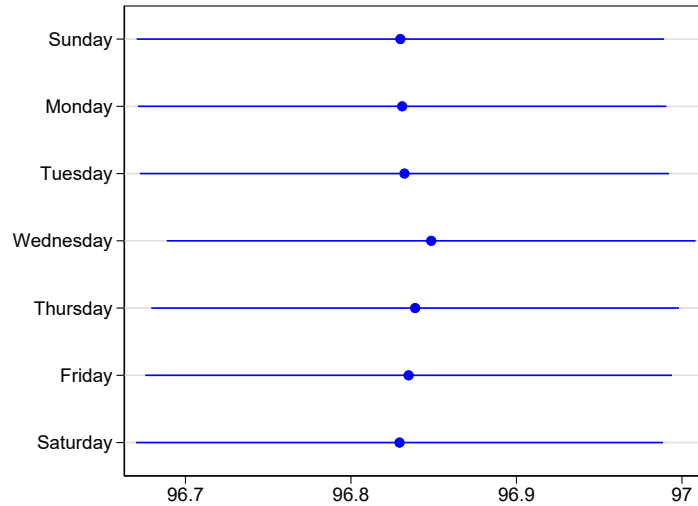


Figure 12: Day of week effects of the Billion Prices Project daily CPI.

B APPENDIX: IMPULSE RESPONSE FUNCTIONS WITH OTHER SHOCKS

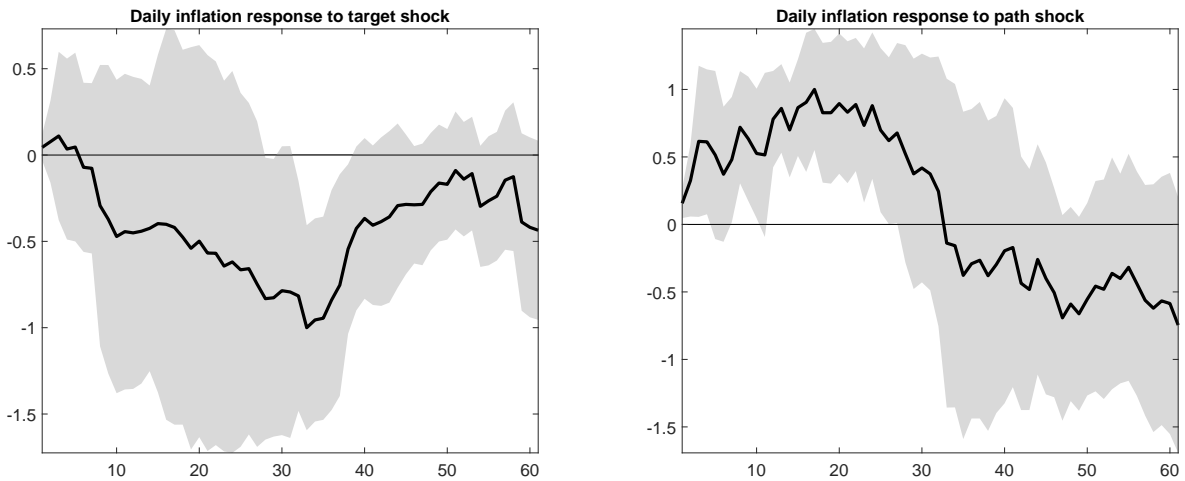


Figure 13: Impulse responses of daily inflation (30-day percentage change) to one standard deviation Gürkaynak et al. (2005) target and path shocks. Error bands are 90 %.

The impulse response of the target shock (left panel) is similar to that of the NS shock shown in panel 4a. Although there is an initial positive impulse response, it is short-lived and not statistically significant from zero. Meanwhile, the subsequent negative impulse response coefficients are statistically significant with 90 % error bands. By contrast, the impulse response of the path shock (right panel) has a significant adversely-signed response for about 30 days before turning conventionally-signed. The signs of these impulse responses are as expected because the target and path shocks capture surprise changes in the federal funds and forward guidance, respectively. The adversely-signed response, often attributed to the Fed information effect’s central bank signaling, is only detected at higher frequencies when using a shock explicitly designed to capture forward guidance.

C APPENDIX: IMPULSE RESPONSE FUNCTIONS WITH LESS SHRINKAGE

This Appendix shows the impulse responses from the state space model under the assumption of less shrinkage - the prior standard deviation of lagged coefficients is now 0.25×0.99^i , where i is the lag.

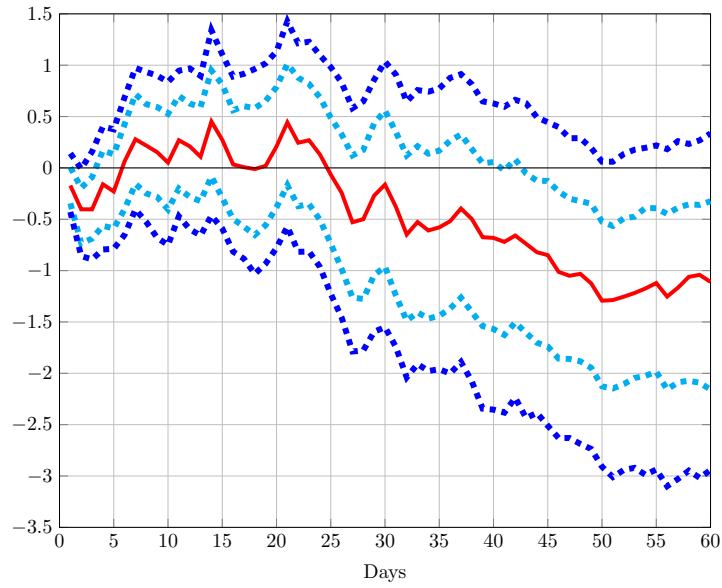


Figure 14: Impulse response of inflation (π_t) to a one standard deviation Nakamura and Steinsson (2018a) monetary policy shock. Error bands are 68 % and 90 % posterior bands centered at the median.

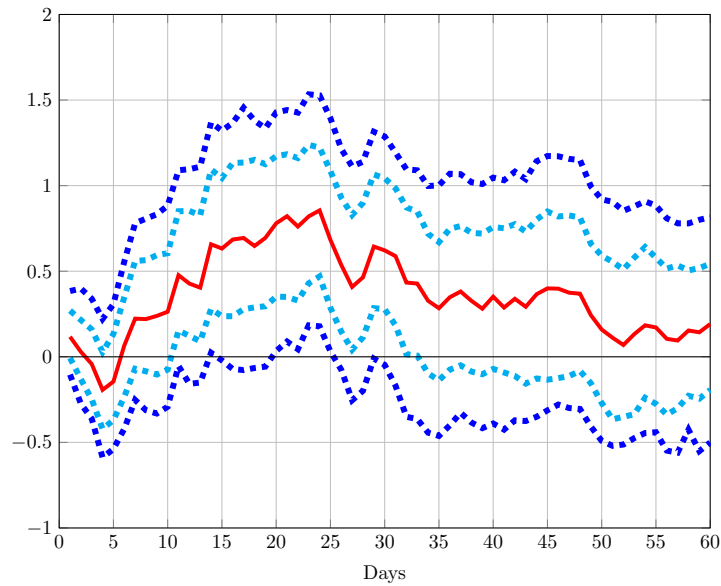


Figure 15: Impulse response of the transitory component of inflation (g_t) to a one standard deviation Nakamura and Steinsson (2018a) monetary policy shock. Error bands are 68 % and 90 % posterior bands centered at the median.

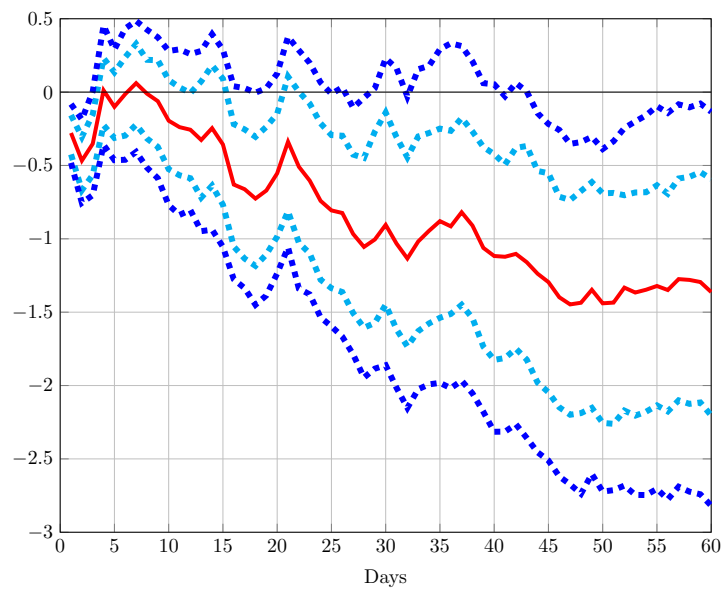


Figure 16: Impulse response of the permanent component of inflation (τ_t) to a one standard deviation Nakamura and Steinsson (2018a) monetary policy shock. Error bands are 68 % and 90 % posterior bands centered at the median.

D APPENDIX: TEMPORAL AGGREGATION

Theorem 1. *The temporally aggregated inflation process given by (3) and (2) satisfies the following two properties:*

1. *The temporally aggregated inflation series, Π_T , follows an ARMA(1,1) process.*

$$(1 - \rho^m L)\Pi_T = u_T + \theta u_{T-1} \quad (6)$$

2. *The innovation of the ARMA(1,1) process (6) is fundamental for the temporally aggregated inflation sequence, Π_T .*

This theorem is well known and dates back to at least to Amemiya and Wu (1972); thus, we do not offer a complete proof but provide intuition and references. To understand part (1), let $\pi_t = \rho\pi_{t-1} + w_t$, where w_t is Gaussian with mean zero and variance $\sigma_w^2 = \sigma_\varepsilon^2/(\phi - \rho)^2$, and note

$$\gamma(0) = \text{Var}(\Pi_T) = \frac{\sigma_\pi^2}{m^2} (m + 2[(m-1)\rho + (m-2)\rho^2 + \dots + \rho^{m-1}]) \quad (7)$$

$$\gamma(s) = \text{Cov}(\Pi_t, \Pi_{t-s}) = \frac{\sigma_\pi^2}{m^2} \rho^{m(|s|-1)+1} (1 + \rho + \rho^2 + \dots + \rho^{m-1})^2 \quad s \neq 0 \quad (8)$$

$$\gamma(s) = \rho^m \gamma(s-1) \quad |s| \geq 2 \quad (9)$$

where $\sigma_\pi^2 = \sigma_w^2/(1 - \rho^2)$, see Wei and Ahsanullah (1984). The intuition of (7)–(8) comes from the correlation structure of an autoregressive process, where all elements are multiplied by $\frac{\sigma_\pi^2}{m^2}$. Thus, there are $(m-1)$ “neighbors”, $(m-2)$ elements two periods removed, etc. Given the strength of the autocorrelation of many macro aggregates, the following limits are useful. As $\rho \rightarrow 1$, the term in brackets in (7) converges to $m(m-1)/2$ and therefore, $\text{Var}(\Pi_T) \rightarrow \sigma_\pi^2$ and $\text{Var}(\Pi_T) \in (0, \sigma_\pi^2)$. Further, the parenthetic term in (8) converges to m as $\rho \rightarrow 1$, and $\text{Cov}(\Pi_t, \Pi_{t+s}) \rightarrow \sigma_\pi^2$.

	π_t	π_{t-1}	π_{t-2}	\dots	π_{t-m}
π_t	1	ρ	ρ^2	\dots	ρ^{m-1}
π_{t-1}	ρ	1	ρ	\dots	ρ^{m-2}
π_{t-2}	ρ^2	ρ	1	\dots	ρ^{m-3}
\vdots					
π_{t-m}	ρ^{m-1}	ρ^{m-2}	ρ^{m-3}	\dots	1

The covariance difference equation (9) identifies the autocorrelation coefficient of the Π_T process as ρ^m . We can then multiply $[(1 - \rho^m L)/(1 - \rho L)] \sum_{j=0}^{m-1} L^j$ to both sides of π_t to give,

$$\left(\frac{(1 - \rho L)(1 - \rho^m L) \sum_{j=0}^{m-1} L^j}{1 - \rho L} \right) \pi_t = \left(\frac{(1 - \rho^m L) \sum_{j=0}^{m-1} L^j}{1 - \rho L} \right) w_t$$

$$(1 - \rho^m L)\Pi_T = \sum_{j=0}^{m-1} (\rho L)^j w_t = u_T + \theta u_{T-1} \quad (10)$$

where $u_T \sim N(0, \sigma_u^2)$. The errors defined by the m moving-average terms $\sum_{j=0}^{m-1} (\rho L)^j w_t$ are correlated and therefore cannot be used to obtain the Wold innovations associated with predicting Π_T linearly from its past. Theorem 1 of Amemiya and Wu (1972) proves that with $m \geq 2$, then the moving-average terms are at most of order one, which establishes the final equality.

The proof of Part 2 also relies on arguments in Amemiya and Wu (1972). In order for the process to be fundamental, one must show that the roots of $1 - \theta z$ lie outside of the unit circle (i.e., $|\theta| < 1$). Given that the initial AR(1) process is positive definite ($\rho \in (0, 1)$), then it has a positive spectral density. As shown in Amemiya and Wu (1972), temporal aggregate maintains the positive definite structure and hence the roots of the moving-average representation must lie outside the unit circle.

D.1 MOVING-AVERAGE FILTERS Suppose we have a stationary stochastic process x_t that is aggregated according to

$$X_T = \left(\frac{1}{m}\right) \left(\sum_{j=0}^{m-1} L^j\right) x_{mT} = \left(\frac{1}{m}\right) (x_{mT} + x_{mT-1} + \dots + x_{mT-m+1}) \quad (11)$$

Note that $1 + L + L^2 + \dots + L^{m-1} = (1 - L^m)/(1 - L)$. Thus, the covariance generating function of X_T is related to x_t by

$$g_X(z) = \frac{1}{m^2} \left(\frac{1 - z^m}{1 - z}\right) \left(\frac{1 - z^{-m}}{1 - z^{-1}}\right) g_x(z) \quad (12)$$

In the frequency domain ($z = e^{-i\omega}$),

$$\begin{aligned} g_X(e^{-i\omega}) &= \frac{1}{m^2} \left(\frac{1 - e^{-i\omega m}}{1 - e^{-i\omega}}\right) \left(\frac{1 - e^{i\omega m}}{1 - e^{i\omega}}\right) g_x(e^{-i\omega}) \\ &= \frac{1}{m^2} \left(\frac{1 - \cos(\omega m)}{1 - \cos(\omega)}\right) g_x(e^{-i\omega}) \end{aligned} \quad (13)$$

where $(1 - e^{-i\omega m})(1 - e^{i\omega m}) = 2 - (e^{i\omega m} + e^{-i\omega m}) = 2 - 2\cos(\omega m) = 2(1 - \cos(\omega m))$ because $e^{i\omega m} = \cos(\omega m) + i\sin(\omega m)$ and $e^{-i\omega m} = \cos(\omega m) - i\sin(\omega m)$. Plotting this function over the range of $[0, \pi]$ gives panel 9b.

E APPENDIX: DATA

This section lists the source and description of each series used in this paper.

OFFICIAL CPI INDEX Analysis in section 2.2 use the BLS' seasonally adjusted Consumer Price Index (FRED: CPIAUCSL) at a monthly frequency. Results in section (3) use the seasonally adjusted (PCPI) and not seasonally adjusted (CPIN) real-time Consumer Price Index which is accessed via the Real-time Data Research Center at the Federal Reserve Bank of Philadelphia.¹⁹ In each real-time spreadsheet, the columns are the date of the vintage and the rows are the time series for that vintage. We then construct a time series by calculating the monthly percentage change for the last two entries for each vintage.

DAILY CPI The Billion Prices Project publicly available daily CPI can be obtained via Cavallo and Rigobon (2016) for July 2008 through August 2015.²⁰ The index is not seasonally adjusted constructed from webscraped prices of multichannel retailers that sell both online and offline.

BREAK-EVEN INFLATION RATES 10-year spot breakeven inflation rates are the daily 10-year Treasury yield at constant maturity (FRED: BC_10YEAR) less the daily 10-year TIPS at constant maturity (FRED: TC_10YEAR). These rates are obtained from the U.S. Treasury Department via FRED.

ZERO-COUPON TREASURY YIELDS Continuously compounded zero-coupon yields (mnemonic: SVENYXX) are obtained via the Federal Reserve Board.²¹

NAKAMURA AND STEINSSON (2018A) **MONETARY POLICY SHOCK** High-frequency monetary policy shocks are originally available from 1995 to 2014.²² We extend this shock series from 1994 to present using futures tick data accessed via CME Group Inc. DataMine (<https://datamine.cmegroup.com/>) at the Federal Reserve Board.²³ The construction of the shock series follows that of Gürkaynak et al. (2005) as described in Nakamura and Steinsson (2018a) and Brennan et al. (2024). The shocks are the first principal component of changes in high-frequency federal funds rate futures and Eurodollar futures:

¹⁹We thank Tom Stark for help obtaining these series. <https://www.philadelphiafed.org/surveys-and-data/real-time-data-research/real-time-data-set-full-time-series-history>

²⁰Series `indexCPI` for `country==USA` in spreadsheet `pricestats_bpp_arg_usa.csv` in folder `all_files_in_csv_format.zip` at website <https://dataverse.harvard.edu/dataset.xhtml?persistentId=doi%3A10.7910%2FDVN%2F6RQCRS>. Alternatively, the data are also available from the `pricestats_bpp_ar_usa.dta` file in the `RAWDATA` folder on the website <https://www.openicpsr.org/openicpsr/project/113968/version/V1/view>.

²¹See https://www.federalreserve.gov/data/yield-curve-tables/feds200628_1.html or as a `csv` file.

²²Series `FFR_shock` from the spreadsheet `PolicyNewsShocksWeb.xlsx` <https://eml.berkeley.edu/~jsteinsson/papers/PolicyNewsShocksWeb.xlsx>

²³<https://eml.berkeley.edu/~jsteinsson/papers/realratesreplication.zip>

$$MP1_s = \begin{cases} \frac{D^s}{D^s - d^s} (ff_{s,t}^1 - ff_{s,t-\Delta t}^1) & \text{if } D^s - d^s > 7 \\ ff_{s,t}^2 - ff_{s,t-\Delta t}^2 & \text{otherwise} \end{cases} \quad (14)$$

$$MP2_s = \begin{cases} \frac{D^{s'}}{D^{s'} - d^{s'}} \left[(ff_{s',t}^j - ff_{s',t-\Delta t}^j) - \frac{d^{s'}}{D^{s'}} MP1_s \right] & \text{if } D^{s'} - d^{s'} > 7 \\ ff_{s',t}^{j+1} - ff_{s',t-\Delta t}^{j+1} & \text{otherwise} \end{cases} \quad (15)$$

$$\Delta ed_q^2 = ed_{q,t}^2 - ed_{q,t-\Delta t}^2 \quad (16)$$

$$\Delta ed_q^3 = ed_{q,t}^3 - ed_{q,t-\Delta t}^3 \quad (17)$$

$$\Delta ed_q^4 = ed_{q,t}^4 - ed_{q,t-\Delta t}^4 \quad (18)$$

Let s index the month of the current FOMC announcement and s' index the month of the next FOMC announcement. For example, $s = \text{March 2014}$ and $s' = \text{April 2014}$ for the March 19, 2014 FOMC announcement where s and s' need not be consecutive months. We define t more precisely as 20 minutes *after* the FOMC announcement while $t - \Delta t$ is defined as 10 minutes *before* the FOMC announcement.²⁴ For the March 19, 2014 FOMC announcement which occurred at 14:00, $t = \text{March 19, 2014 14:20}$ and $t - \Delta t = \text{March 19, 2014 13:50}$.

Let ff^j denote the duration j of the federal funds futures contract ff . For example, $j = 1$ denotes the contract expiring in the current month, $j = 2$ the contract expiring next month, etc. For month s , D^s and d^s are the number of total days in the month and the day of the FOMC announcement, respectively. If a monetary policy announcement occurs in the first 23 days of the month, then that month's federal funds future $j = 1$ is used to calculate $MP1_s$. Because the settlement prices are based on the average of the effective overnight federal funds rate in month s rather than the federal funds rate on a specific day, one must correct for time averaging and scale by the inverse of the share of days remaining in the month, $\frac{D^s}{D^s - d^s}$. Otherwise, if the FOMC announcement occurs in the last seven days of the month, next month's future $j = 2$ is used to calculate $MP1_s$.

$MP2_s$ captures the unexpected change in the federal funds futures contracts that expire at the end of month s' which is the month of the next scheduled FOMC meeting. Brennan et al. (2024) show that in practice the next or following month's federal funds future $j = 2, 3$ is used to calculate $MP2_s$.

Because federal funds futures are highly liquid for contracts expiring in the next three months but less liquid for contracts thereafter, researchers use Eurodollar futures to cover the remaining first year of the term structure. Eurodollar futures are listed quarterly and mature in March, June, September, and December. They are an agreement to exchange, on the second London business day before the third

²⁴As shown by Brennan et al. (2024), the windows are not always this precise in practice and we follow the [online Appendix of Nakamura and Steinsson \(2018a\)](#). For the $t - \Delta t$ contract, we use the contract as close to the 10 minutes before the policy announcement as possible and only consider trades on the day in question. For the t contract, we similarly use the contract as close to the 20 minutes after the announcement as possible and consider trades as late as noon on the following day. If there are no eligible trades to consider, the change is set to zero (i.e., we interpret no trading as no price change). We source the time of the announcements from the Federal Reserve Board and then from Gürkaynak et al. (2005) and Bloomberg News Wire. If there is a conflict in announcement times, we follow this order of priority.

Wednesday of the last month of the quarter, the price of the contract minus the three-month US dollar BBA LIBOR interest rate. Because the BBA LIBOR interest rate is discontinued, Eurodollar futures ceased trading in April 2023. Let q index the quarter of the current FOMC announcement and $q + 1$ index the of the next FOMC announcement. For example, $q = 2014:Q1$, $q + 1 = 2014:Q2$, and $q + 2 = 2014:Q3$ for the March 19, 2014 FOMC announcement.

The monetary policy shock is then the first principal component of expressions (14)-(18) scaled so that its effect on one-year nominal Treasury yields is equal to one.

GÜRKAYNAK ET AL. (2005) **MONETARY POLICY SHOCKS** The target and path shocks of Gürkaynak et al. (2005) are constructed using principal component analysis over the same instrument set as Nakamura and Steinsson (2018a)—expressions (14)-(18). Rather than extracting just the first principal component, Gürkaynak et al. (2005) extract the first two principal components. They rotate these principal components so that the second has no effect on the federal funds rate and therefore captures all other surprises related to monetary policy announcements. The first rotated principal component is the target shock and is normalized so that it is one-for-one with the federal funds rate. The second is the path shock which is normalized to be one-for-one with the four-quarter ahead change in the Eurodollar futures ($ed4_s$ in expression (18)).

BU ET AL. (2021) **MONETARY POLICY SHOCK** Daily monetary policy shocks are available from 1994 to 2020.²⁵ This shock series is constructed by a Fama and MacBeth (1973) two-step regression that extracts unobserved monetary policy shocks Δi_s from the common component of the daily change in zero-coupon yields ΔR_s^j .

1. Estimate the responsiveness of zero-coupon yields ΔR_s^j with maturities $j = 1, \dots, 30$ years to policy indicator Δi_s for each monetary policy announcement s via time-series regressions. For maturities $j = 1, \dots, 30$ there will be 30 regressions.

$$\begin{aligned} \Delta R_s^1 &= \alpha_1 + \beta_1 \Delta i_s + \epsilon_s^1 \\ &\vdots \\ \Delta R_s^{30} &= \alpha_{30} + \beta_{30} \Delta i_s + \epsilon_s^{30} \end{aligned}$$

The implementation assumes Δi_s is one-to-one with the daily change in the two-year constant maturity Treasury yield ΔR_s^2 . For each maturity $j = 1, \dots, 30$, the above expression becomes:

$$\Delta R_s^j = \theta_j + \beta_j \Delta R_s^2 + \underbrace{\epsilon_s^j - \beta_j \epsilon_s^2}_{\xi_s^j}$$

The endogeneity arising from $\text{corr}(\Delta R_s^j, \xi_s^j) > 0$ due to $\beta_j \epsilon_s^2$ being a component of ξ_s^j can be reconciled with IV or the heteroskedasticity-based estimator of Rigobon (2003).

²⁵Series BRW_fomc of spreadsheet brw-shock-series.csv <https://www.federalreserve.gov/econres/feds/files/brw-shock-series.csv>

2. Estimate monetary policy shock $\Delta \hat{i}_s$ from repeated cross-sectional regressions of ΔR_s^j on the responsiveness index $\hat{\beta}_j$ for each FOMC announcement s estimated in step 1.

$$\Delta R_s^j = \alpha_j + \Delta i_s \hat{\beta}_j + v_s^j, \quad s = 1, \dots, T \quad \text{FOMC announcements}$$

3. Re-scale the estimated shock $\Delta \hat{i}_s$ by the assumed normalization in step 1. We follow Bu et al. (2021) and use the daily change in the 2-year Treasury, but our results are robust to scaling by the 1-year to match the scaling of the NS monetary policy shocks.